

Palaeobiology of the early Ediacaran Shuurgat Formation, Zavkhan Terrane, south-western Mongolia

Ross P. Anderson, Sean McMahon, Uyanga Bold, Francis A. Macdonald & Derek E. G. Briggs

To cite this article: Ross P. Anderson, Sean McMahon, Uyanga Bold, Francis A. Macdonald & Derek E. G. Briggs (2016): Palaeobiology of the early Ediacaran Shuurgat Formation, Zavkhan Terrane, south-western Mongolia, Journal of Systematic Palaeontology, DOI: [10.1080/14772019.2016.1259272](https://doi.org/10.1080/14772019.2016.1259272)

To link to this article: <http://dx.doi.org/10.1080/14772019.2016.1259272>



Published online: 20 Dec 2016.



Submit your article to this journal [↗](#)



Article views: 48



View related articles [↗](#)



View Crossmark data [↗](#)

Palaeobiology of the early Ediacaran Shuurgat Formation, Zavkhan Terrane, south-western Mongolia

Ross P. Anderson ^{a*}, Sean McMahon^a, Uyanga Bold^b, Francis A. Macdonald^c and Derek E. G. Briggs^{a,d}

^aDepartment of Geology and Geophysics, Yale University, 210 Whitney Avenue, New Haven, Connecticut, 06511, USA; ^bDepartment of Earth Science and Astronomy, The University of Tokyo, 3-8-1 Komaba, Meguro, Tokyo, 153-8902, Japan; ^cDepartment of Earth and Planetary Sciences, Harvard University, 20 Oxford Street, Cambridge, Massachusetts, 02138, USA; ^dPeabody Museum of Natural History, Yale University, 170 Whitney Avenue, New Haven, Connecticut, 06511, USA

(Received 4 June 2016; accepted 27 September 2016)

Early diagenetic chert nodules and small phosphatic clasts in carbonates from the early Ediacaran Shuurgat Formation on the Zavkhan Terrane of south-western Mongolia preserve diverse microfossil communities. Chert nodules contain abundant fragments of organic material, which include organic-walled microfossils and pieces of microbial mats. These fragments are dominated by several *Siphonophycus* species forming a variety of microbial textures. Spheroids such as *Myxococcoides* are of secondary importance but dominate one rock sample. Dispersed phosphatic clasts within the carbonate matrix preserve degraded filaments and spheroids. Petrographic characteristics and the composition of the palaeobiological community are similar to those of early Ediacaran assemblages elsewhere. The presence of *Salome hubeienensis*, previously reported in the Doushantuo Formation of South China and the Krol Group of the Lesser Himalaya, India, and possible multicellular fossils similar to those of Doushantuo, prompts comparisons with the diversity of other biotas, suggesting similarities in regional early Ediacaran communities. The Shuurgat fossils add to the growing evidence for the nature of Ediacaran ecosystems at this critical juncture in Earth history.

Keywords: Ediacaran; Zavkhan Terrane; fossiliferous chert; Mongolia; Proterozoic; Doushantuo Lagerstätte

Introduction

The Ediacaran Period (635–541 Ma) witnessed one of the most critical transitions in the history of life on Earth. Following the environmental upheavals of the preceding Cryogenian Period (Hoffman & Schrag 2002; Rooney *et al.* 2015), the emergence of widespread macroscopic multicellular fossils (Xiao & Laflamme 2009), sometimes with biomineralized parts (Knoll 2003a), constitutes a profound shift from the microbial communities that dominate the fossil record of the previous ~3 billion years (Knoll 2003b, 2014, 2015; Knoll *et al.* 2006; Cohen & Macdonald 2015). Although molecular clock and biomarker data extend metazoan origins deeper into Neoproterozoic time, Ediacaran sequences provide the first robust body fossil evidence for animal life (Erwin *et al.* 2011; dos Reis *et al.* 2015; Gold *et al.* 2016).

Early Ediacaran fossil Lagerstätten offer glimpses of the transition from a microbial world to one with more complex ecosystems that include macroscopic algae and possible metazoans. Early diagenetic cherts, shales and ore-grade phosphorites preserve soft tissues in extraordinary detail on both macroscopic and microscopic scales

(e.g. Xiao *et al.* 1998, 2014a, b; Y. Zhang *et al.* 1998; Xiao 2004; Yuan *et al.* 2011; L. Chen *et al.* 2014; Liu *et al.* 2014; Muscente *et al.* 2015). Eukaryotes, in particular, show a significant increase in disparity, as documented by the diversification of acanthomorphic acritarchs (Y. Zhang *et al.* 1998; Xiao 2004; Grey 2005; Liu *et al.* 2014; Xiao *et al.* 2014a; Cohen & Macdonald 2015), and multicellular forms (Y. Zhang *et al.* 1998; Xiao 2004; Xiao *et al.* 2004, 2014a, b). Some of these acanthomorphs and multicellular fossils have been interpreted as animal resting stages and embryos, respectively, and may represent some of the earliest body fossil evidence for animals (Xiao & Knoll 2000; L. Yin *et al.* 2007; Cohen *et al.* 2009; L. Chen *et al.* 2014).

Here we describe a new assemblage of early Ediacaran fossils from south-western Mongolia preserved in early diagenetic cherts and phosphate clasts in the Shuurgat Formation on the Zavkhan Terrane of south-western Mongolia. We compare the biodiversity and taphonomy of this diverse array of permineralized microbial fossils with others on the Zavkhan Terrane and beyond, notably the Doushantuo Formation of South China and the Krol Group of the Lesser Himalaya, India.

*Corresponding author. Email: ross.anderson@yale.edu

Geological setting

The Neoproterozoic–Palaeozoic transition is recorded in the carbonate dominated Tsagaan-Olom Group and overlying foreland deposits on the Zavkhan Terrane of south-western Mongolia, a fragment of Proterozoic continental crust embedded in the Central Asian Orogenic Belt (CAOB) (Fig. 1) (Bold *et al.* 2016). The Tsagaan-Olom Group consists of the Cryogenian Maikhan-Uul, Taishir and Khongor formations, and the Ediacaran Ol and Shuurgat formations. These strata were accommodated by ~787–717 Ma rifting and record extensive passive margin

sedimentation (Bold *et al.* 2016). Following a late Ediacaran karstic hiatus, the succession was buried by Ediacaran–Cambrian foreland deposits (Smith *et al.* 2016). Carbonates of the Zuun-Arts Formation span the Ediacaran–Cambrian transition and are overlain by mixed siliciclastic-carbonate strata of the Bayangol and Salaagol formations, and siliciclastic rocks of the Khairkhan Formation (Smith *et al.* 2016). Palaeozoic orogenesis resulted in low-grade metamorphism and broad folding on the autochthon (Bold *et al.* 2016). Carbonate strata lack foliation and preserve primary fabrics where dolomitization has not occurred.

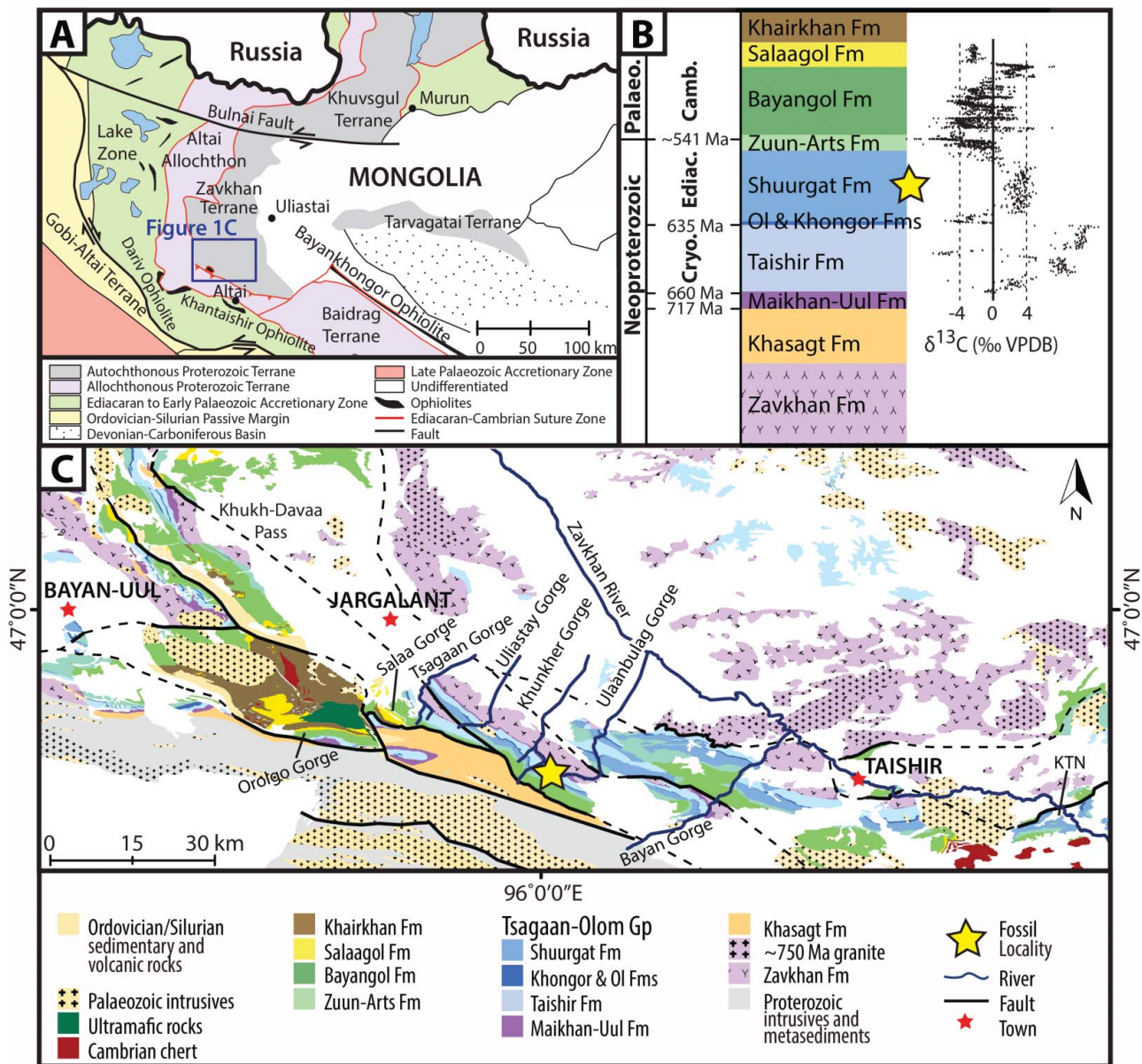


Figure 1. Geological setting of the Shuurgat biota. **A**, map showing Mongolia and Russia, in addition to major tectonic regimes. **B**, generalized stratigraphy of the Zavkhan Terrane, south-western Mongolia; carbon isotopes are plotted for chemostratigraphical correlation globally; yellow star denotes fossiliferous Shuurgat Formation. **C**, geological map of the Zavkhan Terrane with fossil sampling locality denoted by yellow star; adapted from Smith *et al.* (2016).

in graded beds of flat-laminated micritic limestone, variably dolomitized, with minor grain flows of redeposited ooids. Thus, it appears that these strata were deposited in a subtidal environment below fair-weather wave-base. They record shallowing upward through the next ~40 m into a peritidal setting with clear evidence for traction currents and subaerial exposure.

Palaeobiological setting

The Zavkhan Terrane has yielded an array of diverse fossil communities in addition to that described here (Fig. 3). The ~655–640 Ma Taishir Formation preserves unicellular testate fossils in carbonate rocks but multicellular fossils have not been discovered (Bosak *et al.* 2011a, b). Some of these organic microfossils, which are 50–400 μm in maximum dimension, share characteristics with modern agglutinating protists (Bosak *et al.* 2011a, b). The Taishir Formation also hosts macroscopic organic sheets, with ~100 μm tall warty protuberances, identified as possible remnants of marine algae (Cohen *et al.* 2015). These Taishir fossils provide a record of eukaryotic life during the ~660–640 Ma Cryogenian non-glacial interlude, an interval that has yielded few fossils of eukaryotic affinity globally to date (e.g. Anderson *et al.* 2013; Riedman *et al.* 2014; Cohen & Macdonald 2015). Problematic macroscopic structures, described as remains of colonial microorganisms, have been recovered from the underlying Sturtian-equivalent glaciogenic Maikhan-Uul Formation (Serezhnikova *et al.* 2014).

Putative sponge spicules from the Zuun-Arts Formation (Brasier *et al.* 1997) were considered to be evidence of some of the oldest fossil animals, but their nature and even biogenicity have been questioned (C.-M. Zhou *et al.* 1998). More recently, macroscopic Burgess Shale-type carbonaceous compressions of possible marine algae have been reported from this formation (Dornbos *et al.* 2016). Additional diversity is known from silicified phosphatic sediments at the base of the Zuun-Arts Formation, above a regional stratigraphical marker horizon of *Boxonia* stromatolites. Preliminary studies have reported diverse microbial communities dominated by prokaryotic fossils but also including acanthomorphic acritarchs and multicellular forms (Ragozina *et al.* 2007, 2010, 2016). Simple bed-planar trace fossils also occur in the Zuun-Arts Formation (Goldring & Jensen 1996; Smith *et al.* 2016).

The most celebrated fossils from the Zavkhan Terrane are diverse Cambrian small shelly fossils and archaeocyathid patch reefs (e.g. Korobov & Missarzhevsky 1977; Korobov 1980; Voronin *et al.* 1982; Endonzhamts & Lkhasuren 1988; Gibsher & Khomentovsky 1990; Dorjnamjaa & Bat-Ireedui 1991; Gibsher *et al.* 1991; Dorjnamjaa *et al.* 1993; Ushatinskaya 1993; Wood *et al.* 1993; Astashkin *et al.* 1995; Brasier *et al.* 1996; Esakova &

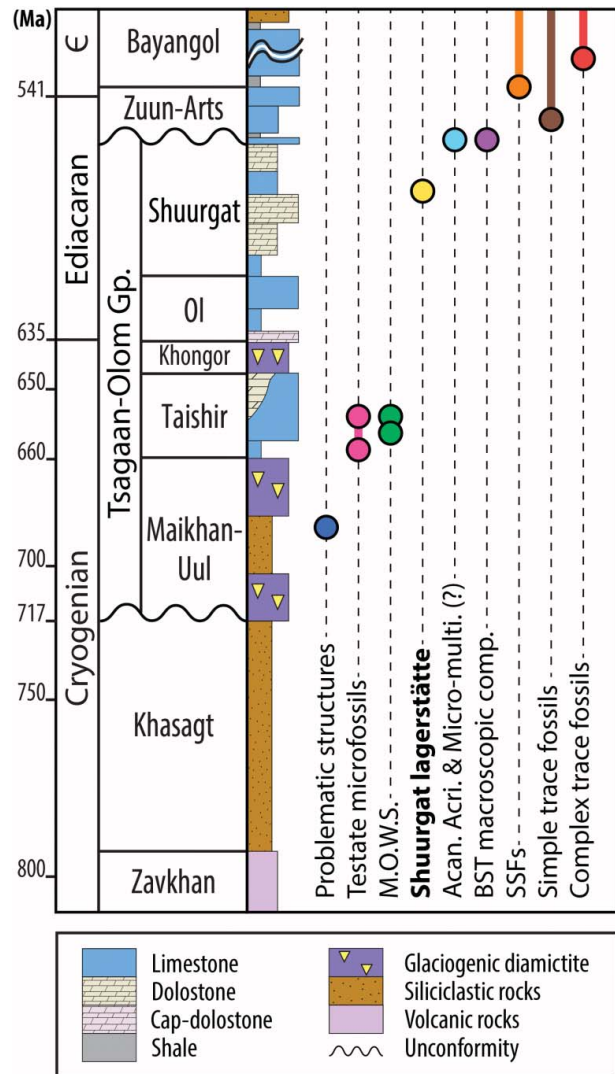


Figure 3. Palaeobiology of the Zavkhan Terrane. Occurrences and stratigraphical ranges (solid bars) of the known fossil assemblages from the Zavkhan Terrane. Plotted against a generalized stratigraphy (Bold *et al.* 2016; Smith *et al.* 2016) are: problematic structures (Serezhnikova *et al.* 2014); testate microfossils (Bosak *et al.* 2011a, b); macroscopic organic warty sheets (M.O.W.S.) (Cohen *et al.* 2015); Shuurgat Lagerstätte (this study); possible acanthomorphic acritarchs and multicellular microfossils including mat communities not dissimilar to those of this study (Ragozina *et al.* 2007, 2010, 2016); Burgess Shale Type (BST) macroscopic organic compressions (Dornbos *et al.* 2016); and small shelly fossils, and simple/complex trace fossils (Smith *et al.* 2016).

Zhegallo 1996; Goldring & Jensen 1996; Khomentovsky & Gibsher 1996; Kruse *et al.* 1996; Lindsay *et al.* 1996; Maloof *et al.* 2010; Smith *et al.* 2016). A recent review refines the distribution of these fossils such that the Bayangol and Salaagol formations yield anabaritids, protoconodonts, cap-shaped fossils, *Salanacus*, hyolithelminthes, coeloscleritophorans, tomotiids, orthothecimorphs, molluscs and calcareous brachiopods, as well as

a variety of trace fossils (Smith *et al.* 2016). Archaeocyathids are confined to the Salaagol Formation (Smith *et al.* 2016). The Bayangol and Salaagol formations also host a variety of complex trace fossils (Goldring & Jensen 1996; Smith *et al.* 2016).

Material and methods

All rock samples and corresponding thin sections are deposited in the collections of the Yale Peabody Museum of Natural History (YPM) Division of Invertebrate Paleontology. YPM collection numbers and sample identifications are given for each rock sample, thin section, and figured microfossil or population.

Three rock samples of the Shuurgat Formation were collected from the base of member Sh3 in the vicinity of Khunkher Gorge (Figs 1 and 2; 46°43'43.697"N, 96°0'30.575"E) and each proved fossiliferous (YPM 534014, RPA1401-1; YPM 534015, RPA1401-2; YPM 534016, F726-165A). The samples were collected from a thin stratigraphical interval (<5 m) or from float derived from the lowermost carbonate beds of Sh3. Thousands of fossils were examined via 30 µm thick polished petrographic thin sections cut subperpendicular to bedding. A single thin section (YPM 534017, RPA1401-1) was obtained from sample YPM 534014 (RPA1401-1). Two thin sections (YPM 534018, F726-165A-A and YPM 534019, F726-165A-B) were obtained from different chert nodules within a 10 cm² area of sample YPM 534016 (F726-165A). Seven thin sections (YPM 534020, RPA1401-2; YPM 534021, RPA1401-2a; YPM 534022, RPA1401-2b; YPM 534023, RPA1401-2c; YPM 534024, RPA1401-2d; YPM 534025, RPA1401-2e; YPM 534026, RPA1401-2f) were obtained from a variety of chert nodules (YPM 534020, RPA1401-2 and YPM 534026, RPA1401-2f from the same large chert nodule) from sample YPM 534015 (RPA1401-2).

Photomicrographs were obtained using a Leica DM 2500 P petrographic microscope combined with a Jenopik CF scan camera, which allows multiple images at higher magnification to be combined. Cathodoluminescence microscopy was carried out using a Reliotron Cathodoluminoscope attached to a Wild M400 Photomicroscope and SPOT Flex camera. Operating conditions were 8 to 9 kV with a 0.5 mA beam current.

Dimensions were measured on fossils encountered along random linear transects of the thin sections. All available specimens of a taxon were measured across multiple thin sections unless hundreds of individuals were available, in which case a representative-sized sample was selected. A statistical method for likelihood-based model selection (Bayesian information criteria, BIC) was used in the package MCLUST in the statistical software R (Fraley & Raftery 2007; R Development Core Team

2010) to identify the most likely number of size modes in the population of *Siphonophycus* (see Darroch *et al.* 2013 and references therein).

Petrography and taphonomy of fossiliferous cherts and phosphatic clasts

Shuurgat microfossils are preserved in early diagenetic black chert nodules and small phosphatic clasts within a bedded, finely crystalline carbonate matrix in which detrital grains such as quartz are rare. The matrix is composed largely of dolomite with minor calcite and phosphate and rare detrital silicates. Petrographic examination revealed that this matrix is predominantly micritic, with areas of silt-sized carbonate grains, variable amounts of phosphate, local concentrations of interstitial silica, occasional linear arrays of dark organic matter that are not always parallel to bedding, and some small (100s of µm) sub-rounded white chert nodules. These small chert nodules contain little organic material and no microfossils, and the cement is chalcedony.

Chert nodules. Chert nodules that preserve organic matter are abundant. Compaction and deflection of laminae below the chert nodules and draping above them (Fig. 4A) suggest that the nodules formed during early diagenesis. The chert nodules are composed predominantly of micro- to meso-crystalline quartz, have sharply defined margins, and fall into two broad categories.

Nodules in Category 1 (mm to cm scale and sub-rounded to rounded, e.g. Fig. 4B) are light in colour with low concentrations of organic matter. They often contain botryoidal silica cements with thicknesses on the order of 10–50 µm (Fig. 4D). The botryoidal growths may nucleate on organic material, including microorganisms, and they occasionally fill cavities in the surrounding carbonate matrix. These organic-poor cherts occur in a distinctive dark-coloured, finely crystalline carbonate matrix, commonly displaying sub-mm scale crinkly laminae. This matrix is partially silicified with abundant phosphate in clasts and linear arrays, and also disseminated finely throughout the matrix (Fig. 5A, B).

The preserved organic matter within these chert nodules is dominated locally by *Myxococcoides* (Fig. 6), numbering in the 100s–1000s and closely packed in clumps. Where pervasive, these microfossils can form the fabric of the organic matter. Organic matter also occurs as amorphous clots. Occasionally, microfossils are present in the silicified portions of the surrounding matrix.

Chert nodules in Category 2 (cm scale and rounded, e.g. Fig. 4C) are black, organic-rich and waxy. They contain a higher concentration of organic matter than Category 1, but the matrix surrounding the nodules is lighter in colour and contains less phosphate. The sharply defined margins

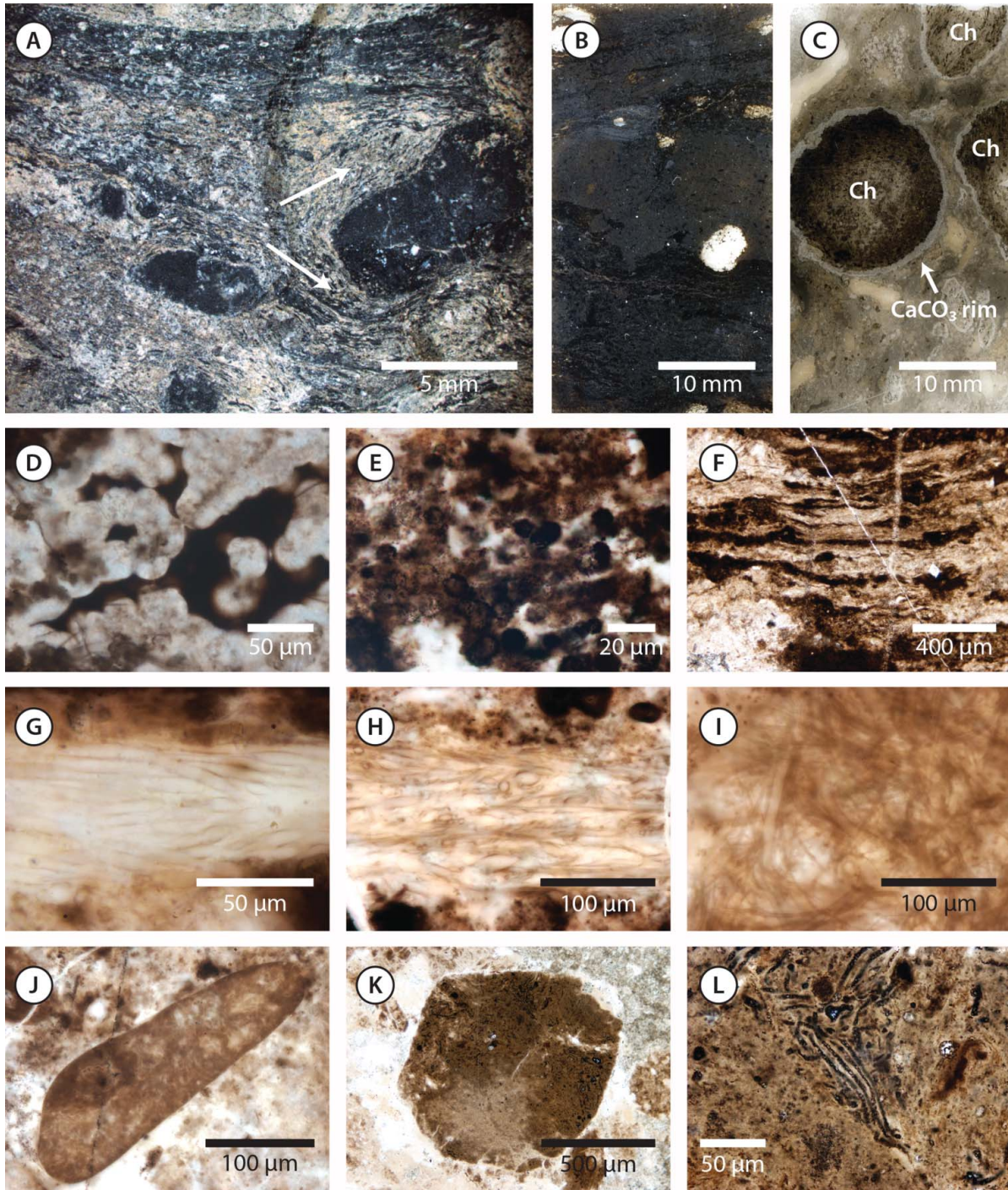


Figure 4. Photomicrograph overviews of the Shuurgat biota. **A**, multiple focal-plane stacked image of rock sample showing fossiliferous chert nodules within carbonate matrix; arrows denote deflection of matrix carbonate laminae around black chert nodule; YPM 534014, RPA1401-1. **B**, Category 1 chert nodules surrounded by heavily phosphatized dark matrix; YPM 534017, RPA1401-1. **C**, Category 2 chert nodules (Ch), often with calcite rims (CaCO_3 rim), and matrix with phosphatization limited to small clasts; YPM 534020, RPA1401-2. **B** and **C** are flatbed-scanned images of thin sections. **D**, botryoidal growth of chert; YPM 534027, RPA1401-1, N75/0. **E**, microbial mat composed of multiple specimens of *Myxococcoides* sp. indet.; YPM 534028, RPA1401-1, B74/0. **F**, layered mat textures; YPM 534046, RPA1401-2a, X59/0. **G**, layered *Siphonophycus typicum* mat; YPM 534047, RPA1401-2a, D62/0. **H**, layered interwoven mat of various *Siphonophycus*; YPM 534041, RPA1401-2, Z62/2. **I**, *Siphonophycus* mat showing criss-crossing texture; YPM 543056, RPA1401-2c, N41/3. **J**, clast of allochthonous microbial mat; YPM 534052, RPA1401-2b, O45/3. **K**, phosphatic clast within matrix containing degraded microfossils; YPM 534048, RPA1401-2a, B48/0. **L**, various unnamed fossils within a phosphatic clast; YPM 534049, RPA1401-2a, B48/1. In this and **Figures 5–9** YPM numbers are given, in addition to rock sample/thin section identifications and, where appropriate, England Finder coordinates for all illustrated sedimentary structures, microfossils and populations.

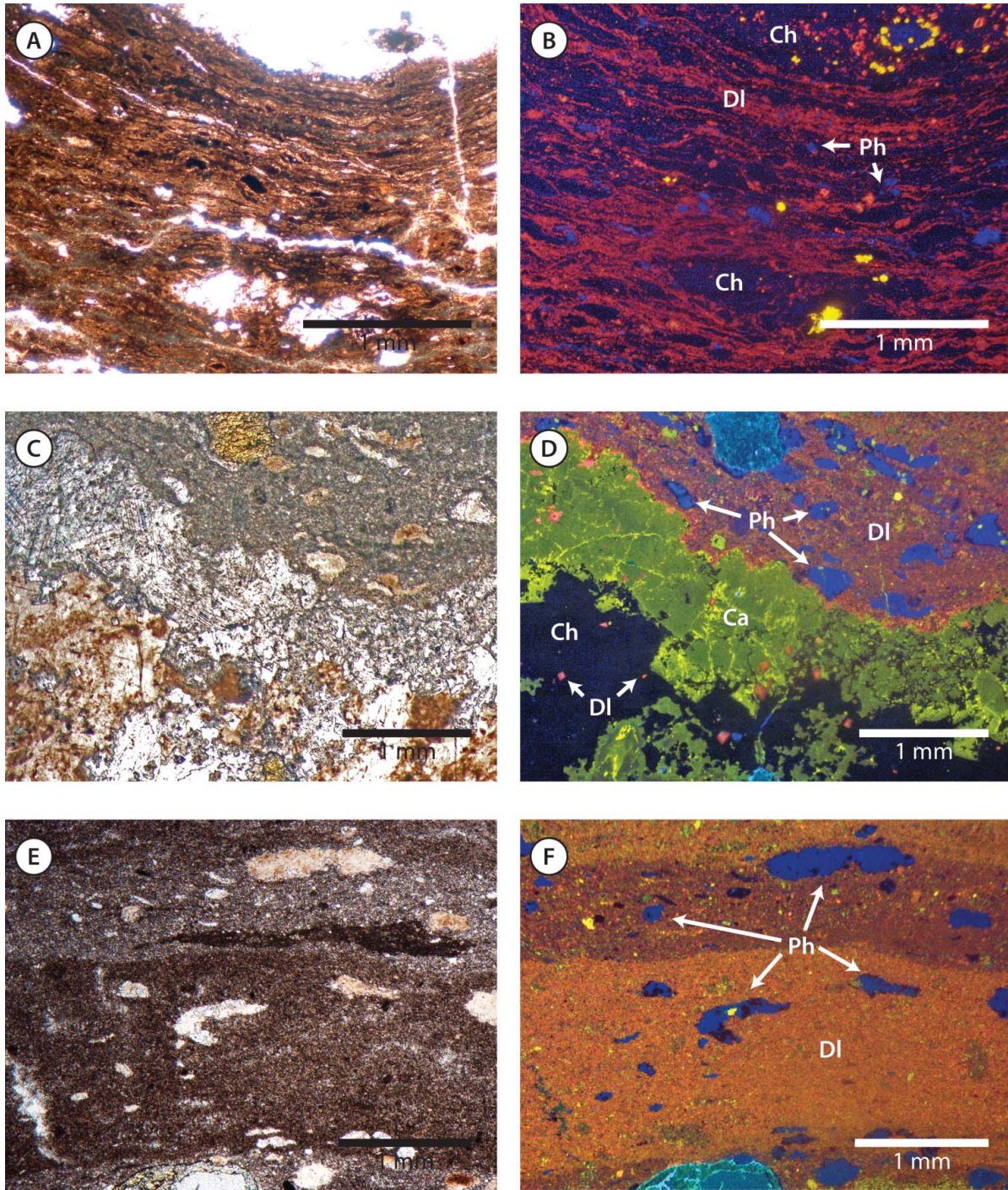


Figure 5. Cathodoluminescence of Shuurgat cherts and phosphatic clasts. **A**, plain light photomicrograph of darker silicified and phosphatic matrix; **B**, cathodoluminescence photomicrograph of same area; organic-lean Category 1 chert nodule (Ch) in top right (black/dark blue); matrix comprises dull-luminescent, red finely crystalline dolomite (DI) with disseminated phosphate (Ph) as well as clasts and linear arrays of phosphatic material; phosphatic material is bright blue; isolated calcite grains are also observed (bright to dull, blotchy yellow); YPM 534017, RPA1401-1, V48/1. **C**, plain light photomicrograph of Category 2 chert nodule boundary; **D**, cathodoluminescence photomicrograph of same area; organic-rich chert nodule (Ch) is non-luminescent (black) with isolated bright-luminescent red dolomite (DI) rhombs; sparry to bladed calcite (Ca) rim is shown luminescing bright to dull, blotchy yellow; matrix is defined by dull-luminescent, red finely-crystalline dolomite (DI) with clasts of phosphatic material (bright blue, Ph); YPM 534024, RPA1401-2d, O47/4. **E**, plain light photomicrograph of phosphatic clasts within carbonate matrix; **F**, cathodoluminescence photomicrograph of same area; phosphatic clasts (blue, Ph) are distinguished from the predominantly red, dull-luminescent dolomitic (DI) matrix; minor bright-luminescent yellow, subhedral calcite also forms part of the matrix and is occasionally present in phosphatic clasts; YPM 534024, RPA1401-2d, V52/0.

of the nodules are often characterized by a rim (~1 mm maximum thickness) of sparry bladed to equant calcite, with crystals up to ~1 mm in length (Figs 4C, 5C, D). The calcite crystals may have more bladed, euhedral faces projecting inward toward the centre of the chert nodule, suggesting that they formed during an episode of de-silicification postdating deposition. Small (<100 µm maximum dimension) clusters and isolated euhedral dolomite rhombs occur sporadically within the nodules, overprinting both chert and calcite (Fig. 5C, D). Similar carbonate rims and dolomite rhombs have been reported in association with lower (Member II and lower strata of Member III) Doushantuo (South China) chert nodules of similar age (Y. Zhang *et al.* 1998; Xiao *et al.* 2010). However, a layer of pyrite often separates the calcite rim from the chert nodules in Doushantuo examples (Xiao *et al.* 2010), a feature that we have not observed in the Shuurgat Formation.

Nodules in Category 2 are dominated by irregular clots of organic matter with scattered microfossils. Occasional *in situ* accumulations are present of laminated microbial mat about 1 mm thick and made up of individual laminae 10s of µm thick. The laminae comprise alternating layers of *Siphonophycus* (Fig. 4F–H) (the tubes usually oriented parallel to the laminae), and darker amorphous organics. Both monospecific (Fig. 4G) and mixed (Fig. 4H) mats are present, but the latter are usually not as extensive and are rarely stacked (in contrast to Fig. 4F). Mats are commonly preserved at an angle to bedding, possibly reflecting disruption and destabilization of the microbial community prior to fossilization. *Salome hubeiensis* (Fig. 7) forms a much rarer component of these communities. *Siphonophycus* also occurs in clumps, with individuals interwoven and criss-crossing each other (Fig. 4I). The preservation of *Siphonophycus* within the microbial mats varies. In some cases, the cell walls appear thicker as a result of degradation (e.g. Fig. 8C, G, J). *Siphonophycus* tubes with thicker walls, however, commonly occur in association with exceptionally preserved examples. Clearly, the silicification that ensured the stability of the microfossils on a geological timescale was preceded by a degree of decay of some individuals.

Rounded intraclasts of microbial mat several hundred µm in maximum dimension are a common constituent of the chert nodules in Category 2 (Fig. 4J). They are predominantly composed of *Siphonophycus septatum* and *S. robustum* (often criss-crossing and interwoven at random angles, resulting in a clumped mat morphology), although examples of *S. typicum* and *S. kestron* are occasionally observed. The microfossils suffered some degradation prior to fossilization (evidenced by less-distinct margins) and this, together with the rounded nature of the mat clasts, suggests that they may have been transported.

In addition to these microbial mat textures, acritarchs infilled with botryoidal silica growths occur in Category 2 chert nodules (Fig. 9E–G).

Phosphatic clasts. Small sub-rounded to rounded dark brown phosphatic clasts (on the order of 10s to 100s µm maximum dimension) occur sporadically within the finely crystalline carbonates that host the chert nodules (Figs 4K, L, 5E, F). Of note is rock sample YPM 534014, RPA1401-1 where phosphatization is not confined to clasts but is pervasive throughout the matrix (Figs 4B, 5A, B). A thin layer of silica cement surrounds some of the clasts, suggesting that phosphatization may have preceded silicification. Phosphate is common in the overlying late Ediacaran Zuun-Arts and Cambrian Bayangol formations (Smith *et al.* 2016) and in coeval strata on the Khuvsgul Terrane of northern Mongolia (Macdonald & Jones 2011), but this is the first report of phosphatic sediments in early Ediacaran Mongolian strata. Organic-rich material may have provided a locus for phosphate mineralization during decay (Briggs & Kear 1993; Briggs 2003; Schiffbauer *et al.* 2014). As such the phosphatic clasts may represent original clasts of organic material within the carbonate matrix that were preferentially phosphatized during diagenesis. Phosphatic sediments are known to promote exceptional preservation in other terminal Proterozoic sequences such as the Doushantuo Formation (e.g. Xiao *et al.* 1998, 2004; Y. Zhang *et al.* 1998; Xiao & Knoll 2000; Schiffbauer *et al.* 2014).

The Shuurgat phosphatic clasts often contain microfossils (e.g. Fig. 4L). The clasts that preserve microfossils tend to be slightly darker in colour. The communities comprise filaments and spheroids, which often occur as isolated individuals in close proximity but not criss-crossing or woven together in a mat texture. Preservation within the phosphatic clasts differs from that in the chert nodules – the organic matter is darker and appears more degraded, making taxonomic identification difficult. Phosphatic clasts may have offered less protection from subsequent maturation (e.g. microfossils are adversely affected by diagenesis and metamorphism: Knoll *et al.* 1988) than did the chert nodules.

Systematic palaeontology

Chroococcacean Cyanobacteria

Genus *Eoentophysalis* Hofmann, 1976, emend.
Mendelson & Schopf, 1982

Type species. *Eoentophysalis belcherensis* Hofmann, 1976.

Eoentophysalis belcherensis Hofmann, 1976
(Fig. 9C)

For synonymy see Sergeev *et al.* (2012).

Remarks. We identify spheroidal to ellipsoidal colonial cells, $\sim 10\ \mu\text{m}$ in maximum dimension with thin ($< 1\ \mu\text{m}$) walls, as *Eoentophysalis belcherensis*. The fossils were found in one isolated broadly spheroidal colony ($150\ \mu\text{m}$ in maximum dimension, YPM 534044) in a chert nodule within thin section YPM 534020, RPA1401-2.

Incertae sedis

Genus *Myxococcoides* Schopf, 1968

Type species. *Myxococcoides minor* Schopf, 1968.

Remarks. Spheroidal microfossils of uncertain systematic affinity are assigned to the genus *Myxococcoides* and identified as known species where possible (see Remarks below).

Myxococcoides minor Schopf, 1968
(Fig. 9A, B)

For synonymy see Sergeev *et al.* (2012).

Remarks. *Myxococcoides minor* comprises spheroidal fossils that possess a thin ($< 1\ \mu\text{m}$) cell wall and are $4\text{--}8\ \mu\text{m}$ in maximum dimension. Individuals almost always display an irregularly shaped amorphous inclusion of opaque organic matter ($< 2\ \mu\text{m}$ maximum dimension) at their centre. The fossil was found in a single cluster (YPM 534039) within a silicified portion of the matrix in thin section YPM 534017, RPA1401-1.

Myxococcoides grandis Horodyski & Donaldson,
1980
(Fig. 6G–J)

For synonymy see Sergeev *et al.* (2012).

Remarks. *Myxococcoides grandis* comprises hollow spheroidal to ellipsoidal fossils with thin organic walls ($\sim 1\ \mu\text{m}$) which often show folds or creases. The species ranges in maximum dimension from 5 to $45\ \mu\text{m}$ with a slight left skew to the size distribution (Fig. 6K). Very rare examples reach larger sizes of up to $115\ \mu\text{m}$ (only three of the 151 sampled exceed $45\ \mu\text{m}$ in diameter) and these may not represent the same species. Individuals of *M. grandis* ($150\text{--}200$ specimens) are found in thin section YPM 534017, RPA1401-1 in discrete associations of a few cells or occasionally in isolation.

Myxococcoides sp. indet.
(Figs 4E, 6A–E)

Remarks. Spheroidal structures $5\text{--}12\ \mu\text{m}$ (mean = $7.8 \pm 1.3\ \mu\text{m}$, $n = 222$) in maximum diameter with dark cell walls, often several μm thick with occasional projections (e.g. Fig. 6D). Petrographic examination suggests that

microcrystalline quartz crystals, formed during early diagenesis, caused the displacement of organic matter within the wall, leading to a thickened appearance; the wall structure does not appear to have been complex. The structures are often intimately associated with botryoidal silica growths, where the silica appears to nucleate on the organism. The structures could be diagenetic, but a confined normal size distribution (Fig. 6F) and possible examples of binary fission (Fig. 6E) provide evidence of biogenicity. We therefore include these structures as a single indeterminate species of *Myxococcoides* (based on the size distribution) but acknowledge that they could be explained by the diagenetic redistribution of organic matter. The thickness of the wall and poor preservation prevent an accurate taxonomic assignment.

The fossils are confined to thin section YPM 534017, RPA1401-1, where they are the dominant species (100s of specimens) and form large clusters in Category 1 chert nodules and occasionally in silicified portions of the surrounding matrix. In some places they comprise the fabric of the organic matter within Category 1 chert nodules.

Genus *Salome* Knoll, 1982

Type species. *Salome svalbardense* Knoll, 1982.

Remarks. Tubular Proterozoic fossils with trichomes characterized by multiple sheath layers (up to eight), which are evident in both longitudinal and transverse sections, are assigned to *Salome*, distinguishing them from *Siphonophycus*. Two species are differentiated primarily on maximum cross-sectional diameter. *Salome svalbardense* has an inner sheath diameter of $8\text{--}16\ \mu\text{m}$ and an outer diameter that reaches $65\ \mu\text{m}$ (Knoll 1982). *Salome hubeiensis* has an inner sheath diameter of $20\text{--}60\ \mu\text{m}$ and an outer diameter that reaches $150\ \mu\text{m}$ (Y. Zhang *et al.* 1998). The two species therefore overlap in size. Some authors (Z. Zhang 1984; C. Yin & Liu 1988) have argued for the presence of multiple species in the Doushantuo Formation but Y. Zhang *et al.* (1998) grouped all specimens as a single morphologically variable population of *S. hubeiensis*, arguing that it overlaps in size with *S. svalbardense*. Given that the size distribution of our specimens suggests a single population that encompasses the size range of *S. hubeiensis*, we follow Y. Zhang *et al.* (1998) and assign all our specimens to this species.

Salome hubeiensis Z. Zhang, 1986
(Fig. 7A–E)

For synonymy see Y. Zhang *et al.* (1998).

Remarks. *Salome hubeiensis* occurs in chert nodules in almost all of our Shuurgat thin sections except YPM 534017, RPA1401-1 as rare clusters (several individuals within a $\sim 1\ \text{mm}$ scale area) and isolated individuals.

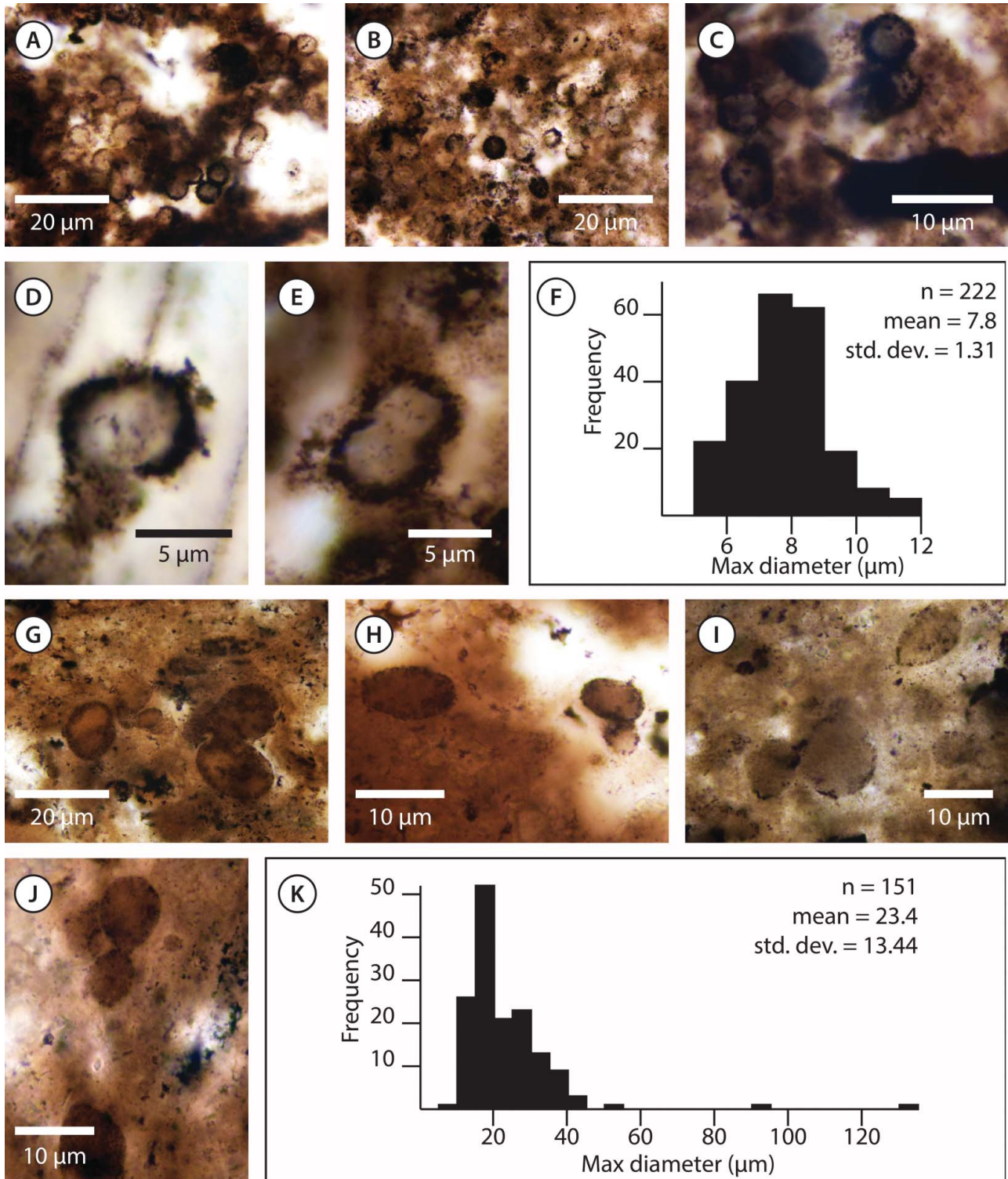


Figure 6. Photomicrographs of *Myxococcoides* with size distributions. **A–F**, primary mat building *Myxococcoides* sp. indet. fossils in Category 1 chert nodules and surrounding silicified matrix; thickened walls reflect dispersion of organic wall through microcrystalline growth of quartz; **A**, YPM 534029, RPA1401-1, T47/3; **B**, YPM 534030, RPA1401-1, V45/1; **C**, YPM 534031, RPA1401-1, B74/0; **D**, YPM 534032, RPA1401-1, J73/2; **E**, potentially records binary fission, YPM 534033, RPA1401-1, B74/0; **F**, histogram of maximum diameter for *M. sp. indet.* **G–K**, rare spherical-ellipsoidal *Myxococcoides grandis*; **G**, YPM 534034, RPA1401-1, C55/0; **H**, YPM 534035, RPA1401-1, C56/1; **I**, YPM 534036, RPA1401-1, H43/0; **J**, YPM 534037, RPA1401-1, X43/0; **K**, histogram of maximum diameter for *M. grandis*.

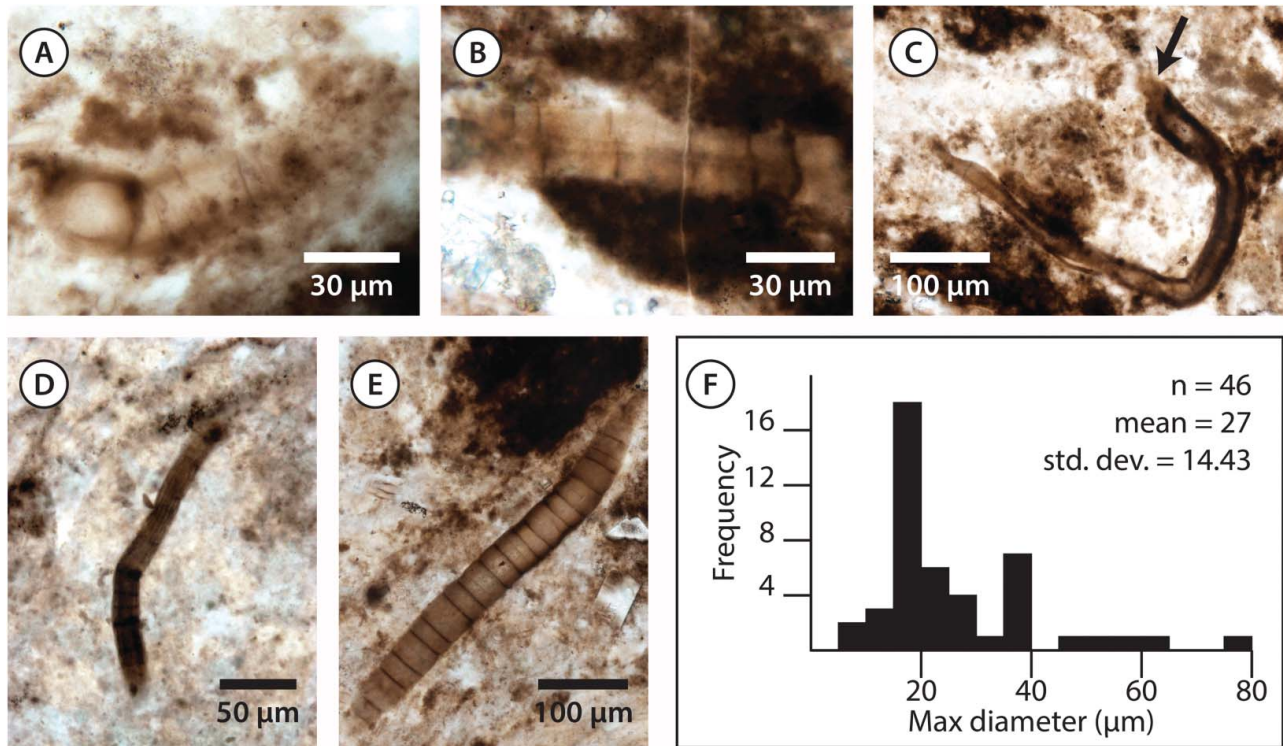


Figure 7. Photomicrographs of *Salome hubeiensis* with size distribution. A–E, *Salome hubeiensis*, showing cross section in A and breaks transversely in B; well-pigmented inner sheath is evidenced in C and D with C also displaying a ‘ruptured’ end (arrow); E shows evidence of trichomes; A, YPM 534061, RPA1401-2e, H51/1; B, YPM 534050, RPA1401-2a, O63/0; C, YPM 534053, RPA1401-2b, O67/1; D, YPM 534042, RPA1401-2, X56/2; E, YPM 534063, RPA1401-2f, F61/2. F, histogram of maximum diameter.

There are ~50 specimens. The sheaths are multilaminar: one end of the specimen in Figure 7A is oriented in a way that provides a cross section revealing at least four sheath laminae. *Salome hubeiensis* is often found twisted and broken transversely into filaments of varying lengths. Occasionally, degradation has occurred at the extremities of the long axis, giving the impression of a ‘rupturing’ termination (Fig. 7C). The filaments are often disrupted, with breaks at irregular intervals that may be offset about the longitudinal axis (Fig. 7B). A well-developed inner sheath encloses a single trichome that is rarely preserved (the trichome was found in <10% of specimens) (Fig. 7E). The wide range in cross-sectional diameter reflects the common loss of outer sheaths which, unlike the inner sheath, are rarely preserved (Y. Zhang *et al.* 1998). In contrast to Doushantuo specimens, the maximum cross-sectional diameter reaches only ~80 µm and many specimens are less than 20 µm, down to a minimum of ~5 µm (Fig. 7F), extending the known size range of this species.

Genus *Siphonophycus* Schopf, 1968, emend. Knoll, Swett & Mark, 1991

Type species. *Siphonophycus kestron* Schopf, 1968.

Remarks. Proterozoic tubular microfossils, which probably represent extracellular sheaths of cyanobacteria, are assigned to *Siphonophycus*, the major microbial mat builder fossilized in Proterozoic successions (e.g. Y. Zhang *et al.* 1998). *Siphonophycus* is abundant in other early Ediacaran successions (e.g. Knoll 1992; Tiwari & Knoll 1994; Y. Zhang *et al.* 1998; Xiao 2004; Liu *et al.* 2014) and it has also been reported from younger units (latest Ediacaran) in the Mongolian sequence (Ragozina *et al.* 2007, 2010, 2016).

Species of *Siphonophycus* are separated on the basis of their maximum cross-sectional diameter (Knoll *et al.* 1991) and diagnosed by dimensions spanning powers of two (1–2, 2–4, 4–8, 8–16, 16–32 µm, etc.). We recovered thousands of specimens from the Shuurgat Formation corresponding in size to at least five of the dimensionally defined species (1–2, 2–4, 4–8, 8–16 and 16–32 µm). However, a size frequency analysis of the maximum diameters of 600 randomly encountered specimens (Fig. 8K) did not identify five distinct biological populations. BIC statistical analysis, plotted as a density function (Fig. 8K, dotted line), reveals that there are most likely three dominant size classes with modes at ~3.4, ~6.5 and ~11.7 µm. The lower two of these three correspond to the reported size classes 2–4 and 4–8 µm. The BIC analysis combines individuals larger than this into

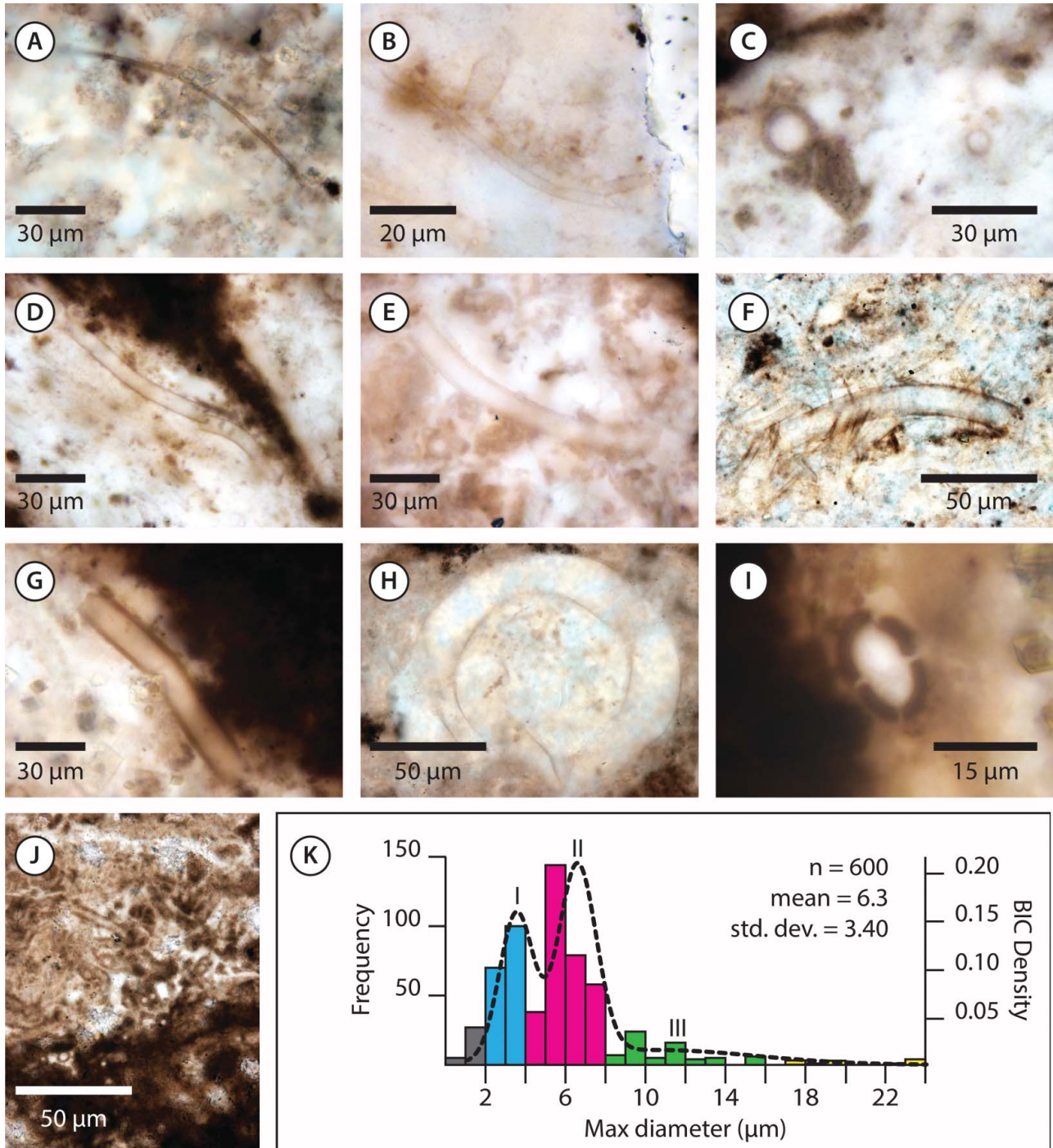


Figure 8. Photomicrographs of *Siphonophycus* with size distribution. **A**, *Siphonophycus septatum*; YPM 534038, RPA1401-1, T50/3. **B**, *Siphonophycus robustum*; YPM 534043, RPA1401-2, P70/4. **C**, *Siphonophycus typicum* and *S. kestron* both in cross section; the cell walls in both instances have degraded to give the appearance of a thickened wall; YPM 534062, RPA1401-2e, J47/1. **D**, *Siphonophycus typicum* showing break/tear transversely in cell; YPM 534054, RPA1401-2b, L46/0. **E**, *Siphonophycus kestron* showing degraded and thickened wall; YPM 534059, RPA1401-2d, J54/4. **F**, *Siphonophycus typicum* and *S. septatum*; YPM 534064, RPA1401-2f, C47/2. **G**, **H**, *Siphonophycus solidum*; **G**, YPM 534065, RPA1401-2f, N37/3; **H**, YPM 534068, F726-165A-B, V42/2. **I**, possible *Siphonophycus* with brittle longitudinal fractures in cell wall; YPM 534057, RPA1401-2c, H42/4. **J**, ghost *Siphonophycus* filaments in poorly preserved setting; YPM 534058, RPA1401-2c, O69/3. **K**, histogram of maximum diameter with ~100 individuals measured per thin section (grey, *S. septatum*; blue, *S. robustum*; magenta, *S. typicum*; green, *S. kestron*; yellow, *S. solidum*); density function (dotted line) from Bayesian information criteria (BIC) is superimposed on histogram showing modal size categories.

a single variable size class, although this class has far fewer representatives (Fig. 8K). It is unclear whether the absence of a clear separation of the larger size classes that have been described in the literature (8–16 and 16–32 μm) is real or simply reflects the small sample size. Neither does the BIC analysis resolve the smallest species (1–2 μm). This taxon has previously been questioned since small specimens could represent a larger species that shrank during diagenesis (Knoll 1981). For consistency with previous work we report all observed size classes, yet note that our analyses suggest that they may not all reflect true biological populations.

Specimens of *Siphonophycus* often show evidence of fracturing/tearing across the long axis (e.g. Fig. 8D). Additionally, we document a single specimen, preserved in cross section, which shows four almost equal longitudinal divisions of the cell wall (Fig. 8I). We tentatively interpret this as a result of brittle fracturing of the cell wall for reasons unknown.

Siphonophycus septatum (Schopf, 1968) Knoll,
Swett & Mark, 1991
(Figs 4H–J, 8A, F)

For synonymy see Butterfield *et al.* (1994).

Remarks. *Siphonophycus septatum* comprises filamentous tubes 1–2 μm in maximum diameter. Within the Shuurgat Formation, *S. septatum* is found within mat clasts, often with its tubes interwoven in a criss-crossing random fashion (as in the ~800 Ma Svanbergfjellet Formation: Butterfield *et al.* 1994), or as isolated filaments. It is present in chert nodules from all rock samples examined and may not be confined to a single ecological niche within the formation.

Siphonophycus robustum (Schopf, 1968), comb.
Knoll, Swett & Mark, 1991
(Figs 4H–J, 8B)

For synonymy see Schopf *et al.* (2015).

Remarks. *Siphonophycus robustum* comprises filamentous tubes 2–4 μm in maximum diameter. It occurs as isolated filaments, often associated with additional specimens in a local (100s of μm) area, and as a major component of microbial mat clasts and laminae. Within mats *S. robustum* is interwoven either in a criss-crossing random fashion or aligned along a single plane defined by sedimentary laminae. It is present in chert nodules from all rock samples examined and may not be confined to a single ecological niche within the formation.

Siphonophycus typicum (Hermann, 1974) comb.
Butterfield in Butterfield, Knoll & Swett, 1994
(Figs 4G–I, 8C, D, F)

For synonymy see Butterfield *et al.* (1994).

Remarks. *Siphonophycus typicum* comprises tubes with a maximum diameter of 4–8 μm . *Siphonophycus typicum* is the most abundant species of *Siphonophycus* preserved within Shuurgat rocks. It is the principal mat builder in both mat clasts and layered microbial laminae, and was observed in chert nodules from all thin sections except YPM 534017, RPA1401-1.

Siphonophycus kestron Schopf, 1968
(Figs 4H, 8C, E, F)

For synonymy see Y. Zhang *et al.* (1998).

Remarks. *Siphonophycus kestron* comprises tubes with a maximum diameter of 8–16 μm . The majority of specimens are <12 μm . It is often found in association with *S. typicum* within clasts and layered microbial mats of the Shuurgat Formation but it also occurs as isolated individuals. The species is present in chert nodules from all thin sections except YPM 534017, RPA1401-1.

Siphonophycus solidum (Golub, 1979) comb. But-
terfield in Butterfield, Knoll & Swett, 1994
(Fig. 8G, H)

For synonymy see Schopf *et al.* (2015).

Remarks. *Siphonophycus solidum* comprises tubes with a maximum diameter of 16–32 μm . The taxon is extremely rare in Shuurgat chert nodules (2% of our random sample of 600 *Siphonophycus* specimens: Fig. 8K), occurring mostly as isolated specimens, although it is occasionally associated and entwined with smaller *Siphonophycus* species.

Filaments (Figs 4L, 9K)

Description. Dark, unbranched organic filaments (<5 μm maximum diameter) are transected along their length at irregular intervals. The organic matter is darker than the Shuurgat *Siphonophycus* tubes described above.

Remarks. The filaments (100s of specimens) are confined to phosphatic clasts (Fig. 4K, L) where they form loose clusters, often at random orientations with respect to each other. They were observed in all thin sections except YPM 534017, RPA1401-1. The filaments resemble those fossilized in Archaean rocks (e.g. Schopf 2006; Knoll 2012, 2015) and the genus *Gunflintia* from the Palaeoproterozoic Gunflint Formation, Ontario, Canada (Barghoorn & Tyler 1965). Given the poor quality of preservation, however, we do not assign a taxonomic name – they could be specimens of *Siphonophycus* tubes with transecting elements generated by degradation and redistribution of organic matter (e.g. Knoll 2012).

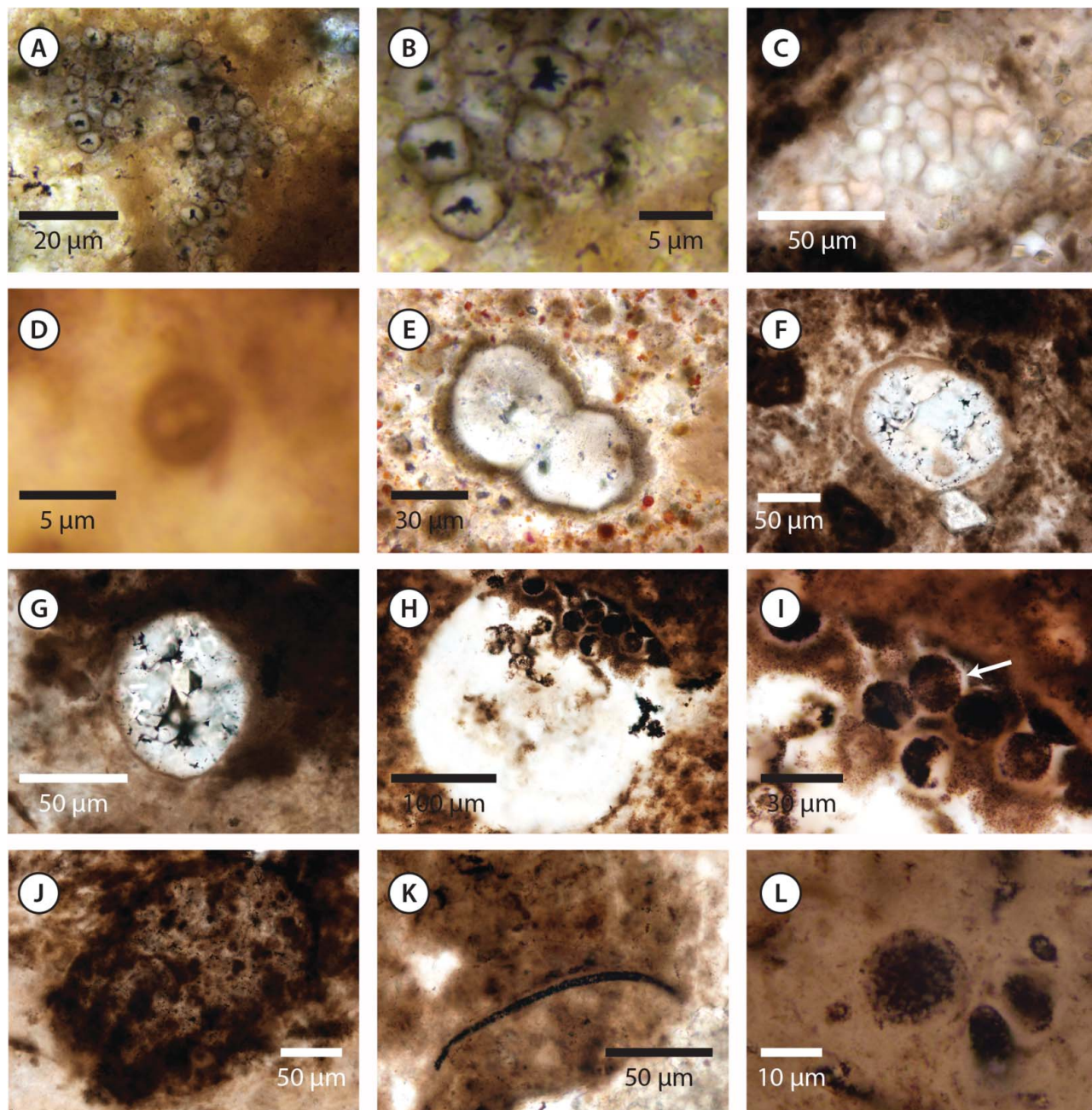


Figure 9. Rare fossils in the Shuurgat Lagerstätte. **A–G**, rare forms from large black chert nodules; **A, B**, *Myxococcoides minor*, YPM 534039, RPA1401-1, P56/0; **C**, *Eoentophysalis belcherensis*, YPM 534044, RPA1401-2, O50/2; **D**, multiple tubes within sheaths (because of the small size of this specimen, imaging was challenging), YPM 534055, RPA1401-2b, U69/3. **E–G**, *Leiosphaeridia* spp., **E** may show binary fission, and **F–G** show silica growths toward the cell centre from the wall; **E**, YPM 534069, F726-165A-B, U54/2; **F**, YPM 534066, RPA1401-2f, S67/3; **G**, YPM 534067, RPA1401-2f, Q36/0). **H, I**, unnamed large spheroidal body, arrow denotes separation of some internal spheres into two halves YPM 534070, F726-165A-B, Y42/2. **J**, unnamed amorphous large structure; YPM 534045, RPA1401-2, C55/4. **K, L**, unnamed forms from phosphatized clasts; **K**, YPM 534060, RPA1401-2d, E62/1; **L**, YPM 534051, RPA1401-2a, B48/0.

Large amorphous structures (Fig. 9J)

Description. Large amorphous structures up to several hundred μm in maximum dimension are preserved in

chert nodules. The structures comprise a thick dark outer envelope $<10\ \mu\text{m}$ in maximum dimension which is very variable in shape. Areas of diffuse dark organic matter occur inside the envelope, often concentrated into solid ovoids $10\text{--}20\ \mu\text{m}$ in maximum dimension.

Remarks. These enigmatic structures are quite degraded, as evidenced by the diffuse organic matter within the thickened, poorly defined envelope. They may represent clusters of small spheroidal unicells enveloped by a sheath, accounting for their variable morphology (e.g. Knoll 2015). Given their rarity (<10 per chert nodule), amorphous nature and poor preservation, we do not assign them to a taxon.

Multiple tubes within sheaths (Fig. 9D)

Remarks. A single specimen preserves two tubular structures (1–2 μm maximum diameter) within an outer tubular sheath (<5 μm maximum diameter). The internal tubes are entwined in a helical manner. Given that we only observed a single specimen we choose not to assign it taxonomically.

Spheroids (Figs 4L, 9L)

Description. Spheroids (100s of specimens) of various sizes (up to 16 μm maximum diameter) are commonly preserved in phosphatic clasts (Fig. 4K, L). The organic matter comprising the spheroids is very dark and is comparable to that making up the filaments described above. The boundary of the spheroids is often diffuse (Fig. 9L).

Remarks. The spheroids, like the filaments from the small phosphatized clasts, are poorly preserved. The diffuse boundaries and dark organic matter suggest some degradation prior to fossilization, or alteration during diagenesis/metamorphism, leading to redistribution of organic matter (e.g. Knoll 2012). There is insufficient information to assign them to a taxon.

Large spheroidal structure with internal spheres (Fig. 9H, I)

Description. A single spheroidal specimen 250 μm in maximum diameter with a sharp boundary was discovered in YPM 534019, F726-165A-B. Enclosed within the large sphere are multiple small rounded spherical bodies, 20–25 μm in maximum diameter. These are only present loosely packed along one margin of the specimen, and they appear degraded. Some appear to be transected by the outer envelope. Organic material of the same dark appearance as these small bodies, but of uncertain morphology, is present elsewhere in the sphere, suggesting that they may have once filled the entire structure. Some of the internal bodies appear to be separated into two halves (Fig. 9I).

Remarks. The specimen resembles the multicellular fossil described as *Megaclonophycus onustus* from the Doushantuo Formation (Xue *et al.* 1995; Xiao & Knoll 2000; Xiao 2004). We follow Xiao *et al.* (2014a, b) in

synonymizing *Megaclonophycus* with *Megasphaera*. *Megasphaera* is globular, with a thin, smooth envelope that in specimens originally described as *Megaclonophycus* encloses hundreds of small (20–40 μm diameter) spherical internal bodies (Xiao & Knoll 2000). It has been interpreted as the remains of sulphur-oxidizing bacteria (Bailey *et al.* 2007), unicellular protists (Bengtson *et al.* 2012), mesomycetozoean-like holozoans (Hultgren *et al.* 2011), *Volvox*-like green algae (Xue *et al.* 1995; Butterfield 2011), and embryos of metazoans or bilaterian animals (Xiao *et al.* 1998; Xiao & Knoll 2000; Hagadorn *et al.* 2006; L. Yin *et al.* 2007; J.-Y. Chen *et al.* 2009; Cohen *et al.* 2009; Z. Yin *et al.* 2013). A recent reexamination of the species, which focused on cell differentiation, considered an affinity with cellularly differentiated multicellular eukaryotes, which include stem-group animals and algae, most likely (L. Chen *et al.* 2014; Xiao *et al.* 2014b). Xiao & Knoll (2000) recognized degraded *Megasphaera* specimens from the Doushantuo Formation (cf. Y. Zhang *et al.* 1998, fig. 13, parts 7–8), but none of those figured show the same degree of degradation as the Shuurgat specimen and they do not provide a basis for effective comparison.

Although the Shuurgat specimen may share an affinity with *Megasphaera* from the Doushantuo Formation, the availability of a single poorly preserved specimen, which shows only a few internal spheroids and provides limited information regarding the outer envelope, prevents a confident assignment. The structure may represent a single large leiosphaerid acritarch infilled with early diagenetic silica (acritarchs infilled with silica occur within Shuurgat cherts, e.g. Fig. 9E–G). The internal spheroids may be diagenetic which might explain why some of them appear to be transected by the outer envelope, a scenario which is unlikely if they were spheroidal cells enclosed by a large biological envelope. Examination of further Shuurgat samples both in thin section and via weak acid maceration (a technique used for Doushantuo fossils) is required to find similar specimens and determine whether this is the first representative of *Megasphaera* to be found outside the Doushantuo Formation or simply an artefact of diagenesis.

Acritarchs

Genus *Leiosphaeridia* Eisenack, 1958
(Fig. 9E–G)

Type species. *Leiosphaeridia baltica* Eisenack, 1958.

Leiosphaeridia spp.
(Fig. 9E–G)

Remarks. Simple spheroidal fossils are placed in the genus *Leiosphaeridia* without differentiating species, following Y. Zhang *et al.* (1998). These fossils are rare in Shuurgat chert nodules (10s of specimens). They are often

infiltrated with silica that precipitated inwards from the organic wall (e.g. Fig. 9G).

Discussion

Palaeoecology

Reconstructing the palaeoecology of Proterozoic microbial communities is challenging due to the difficulty of assigning systematic affinities to many fossils, and limited knowledge of taphonomic biases. Chert commonly only preserves extracellular sheaths, thus providing somewhat limited biological information (Knoll 2012, 2015; Schopf *et al.* 2015), and the majority of cherts represent shallow peritidal environments (Knoll 1985; Maliva *et al.* 1989). However, the study of a single region, through detailed sampling of multiple stratigraphical sections in a palaeo-environmental context with an understanding of taphonomic bias, can reveal palaeoecological information. For example, the composition of microbial communities from the ~760 Ma Draken Formation of Spitsbergen (Knoll 1982) was found to reflect their origin in upper or lower tidal flat, lagoonal and oolitic shoal sedimentary facies, permitting the reconstruction of the ecology of the environmental settings represented by the formation (Knoll *et al.* 1991).

The chert-hosted Shuurgat microfossils likewise hint at differing palaeoecologies. Category 1 chert nodules are dominated by *Myxococcoides* which can form large masses and is also occasionally preserved in silicified portions of the dark, phosphatized matrix that surrounds the nodules. Category 2 chert nodules, in contrast, are dominated by *Siphonophycus*. They yield *Siphonophycus* in small associations of isolated individuals of *S. septatum* and *S. robustum*. These nodules also often contain well-preserved microbial mats composed of *Siphonophycus* filaments, the most fully developed layered examples of which are composed of a single species (usually *S. typicum* or *S. kestron*), whereas smaller mats may be composed of multiple species.

Small rounded intraclasts of *Siphonophycus* mat composed predominantly of interwoven clumps of *Siphonophycus septatum* and *S. robustum*, with occasional *S. typicum* and *S. kestron*, also occur within the Category 2 chert nodules and may represent a third microbial community. These mat fragments may be derived locally and rounded during transportation by a storm event prior to silicification.

Comparison with other early Ediacaran Lagerstätten

The discovery of the Shuurgat Lagerstätte adds to a growing number of early Ediacaran units that preserve fossils in cherts and phosphatic sediments. Some of these other

units preserve possible body fossil evidence of the earliest animals through acanthomorphic acritarchs and multicellular fossils often interpreted either as resting stage cysts or as embryos (Xiao & Knoll 2000; L. Yin *et al.* 2007; Cohen *et al.* 2009; L. Chen *et al.* 2014). The Shuurgat biota shares some characteristics of community composition and taphonomy with two of these units: the Doushantuo Formation (South China) and Krol Group (Lesser Himalaya, India).

The ~635–500 Ma Doushantuo Formation preserves fossils in three broad assemblages: those of its lower (Member II and lower strata of Member III) and upper (Member III) cherts, and those of its phosphorites (Y. Zhang *et al.* 1998; Xiao 2004; McFadden *et al.* 2009; Liu *et al.* 2014; Xiao *et al.* 2014a; Muscente *et al.* 2015). These fossiliferous strata are early Ediacaran in age and are bracketed broadly by Marinoan glacial deposits and the Shuram carbon isotope excursion (Condon *et al.* 2005; Muscente *et al.* 2015). The lowermost Krol A Member of the Krol Group also preserves microfossils in chert nodules at its base (Tiwari & Knoll 1994). These fossils are likewise interpreted to be early Ediacaran in age, based on litho- and chemostratigraphical correlations (Jiang *et al.* 2002; 2003; Valdiya 2016). The fossils were originally thought to be from the underlying Infra Krol Formation (Tiwari & Knoll 1994), but revision of the stratigraphy has assigned them to Krol A (Jiang *et al.* 2002, 2003). In either case, their age remains early Ediacaran as the entire sequence is bracketed by a glacial diamictite below a cap carbonate (Blaini Formation) thought to represent the (~640–635 Ma) Marinoan Snowball Earth glaciation (Jiang *et al.* 2003).

The Shuurgat chert nodules, particularly those in Category 2, share many petrographic characteristics with those of the lower Doushantuo and Krol A. They are similar in overall size and shape (cm scale and ellipsoidal), and in their internal microfabrics which include abundant amorphous organic matter and textures such as layered *Siphonophycus* mats (Tiwari & Knoll 1994; Y. Zhang *et al.* 1998). The Shuurgat and Doushantuo nodules share a carbonate rim ~1 mm thick which, in the case of Doushantuo, is thought to be a product of later diagenesis (Y. Zhang *et al.* 1998; Xiao *et al.* 2010). Such a rim is not documented on Krol A nodules. All three contain scattered small dolomite euhedra (Tiwari & Knoll 1994; Y. Zhang *et al.* 1998), but the Shuurgat nodules differ in lacking small pyrite euhedra.

The Shuurgat (Category 2), Doushantuo and Krol A chert nodules yield similar microfossil communities. All are dominated by *Siphonophycus* which occurs as individuals, loose clusters and complex microbial mats. *Siphonophycus robustum*, *S. typicum*, *S. kestron* and *S. solidum* are present in Doushantuo cherts, with possible occurrences of *S. septatum* (Y. Zhang *et al.* 1998; Xiao 2004; Liu *et al.* 2014). Similarly, *S. robustum*, *S. typicum*

(described as *S. inornatum*) and *S. kestron* are present in Krol A cherts (Tiwari & Knoll 1994). *Myxococcoides* and *Leiosphaeridia* also occur in all three settings (Tiwari & Knoll 1994; Y. Zhang *et al.* 1998; Xiao 2004; Liu *et al.* 2014).

The occurrence of these early Ediacaran *Siphonophycus*, *Myxococcoides* and *Leiosphaeridia* communities does not necessarily imply biostratigraphical equivalence. Each of these form-taxa may represent a number of different biological species, their morphology converging as a result of taphonomic processes (Knoll *et al.* 1991). Moreover, chert nodules hosting such fossils are not confined to early Ediacaran time but occur in a variety of other Proterozoic successions (e.g. Schopf 1968; Knoll *et al.* 1991; Schopf & Klein 1992; Sergeev *et al.* 2012).

An additional morphologically distinct taxon reported here in chert nodules in Category 2, which was previously known only from Doushantuo and Krol A cherts, is *Salome hubeiensis* (Z. Zhang 1986; Tiwari & Knoll 1994; Y. Zhang *et al.* 1998; Liu *et al.* 2014). This species is rare in lower Doushantuo but common in upper Doushantuo and in Krol A cherts (Z. Zhang 1986; Tiwari & Knoll 1994; Y. Zhang *et al.* 1998; Liu *et al.* 2014). Its presence in Doushantuo, Krol A and Shuurgat cherts may reflect coeval deposition, palaeogeographical proximity and/or similar depositional environments. Cherts with similar petrographic characters from a similar palaeodepositional setting in the approximately coeval Scotia Group of Svalbard do not preserve *S. hubeiensis* (Knoll 1992; Y. Zhang *et al.* 1998), suggesting that it is not ubiquitous in early Ediacaran successions globally and may not be a good global biostratigraphical marker. Palaeomagnetic and detrital zircon data suggest that the South China and Indian land masses were in close proximity between 635 and 580 Ma, and collision between the two may have started at this time (Li *et al.* 2013; Yao *et al.* 2014). The palaeogeographical location of the Zavkhan Terrane, which hosts the Shuurgat Formation, however, is unknown. Li *et al.* (2013) placed the Zavkhan Terrane proximal to but northeast of South China/India, with Laurentia (including the Scotia Group that does not preserve *S. hubeiensis*) distal to all three. Consequently, the presence of *S. hubeiensis* in the Doushantuo (South China), Krol A (India) and Shuurgat (Mongolia) cherts, but not in the Scotia Group (Laurentia), may indicate that the species was confined to a regional palaeogeographical area.

In spite of similarities in petrography and biota, the Shuurgat cherts have not yielded many of the taxa in the Doushantuo and Krol A cherts that represent the complex morphologies characteristic of Ediacaran microfossil communities. Both Doushantuo and Krol A cherts yield acanthomorphic acritarchs (Tiwari & Knoll 1994; Y. Zhang *et al.* 1998; Xiao 2004; McFadden *et al.* 2009; Liu *et al.* 2014; Xiao *et al.* 2014a), which occur in Ediacaran successions globally (e.g. Zang & Walter 1992; Grey

2005; Vorob'eva *et al.* 2009; Golubkova *et al.* 2010; Sergeev *et al.* 2011). The absence of such fossils from the Shuurgat cherts may reflect limited sampling. Within the Doushantuo Formation, for example, McFadden *et al.* (2009) reported that acanthomorphic acritarchs comprised only ~3% of 32,719 described fossils from a total of 422 chert nodules in 176 distinct stratigraphical horizons. In comparison, prokaryotic forms accounted for ~85% of the fossils. Indeed, in early studies, prior to more detailed sampling (e.g. McFadden *et al.* 2009), acanthomorphic acritarchs were described as absent from lower Doushantuo cherts, which the Shuurgat cherts most closely resemble petrographically (Y. Zhang *et al.* 1998). Elsewhere on the Zavkhan Terrane, phosphorites of the basal Zuun-Arts Formation (stratigraphically above the Shuurgat Formation and likely late Ediacaran in age: Smith *et al.* 2016), have yielded possible acanthomorphic acritarchs, including examples assigned to *Knollisphaeridium* (described under its former name *Echinosphaeridium* in Mongolia) (Ragozina *et al.* 2007, 2010, 2016), which is also known from the Doushantuo Formation (Xiao 2004; Liu *et al.* 2014).

Acanthomorphic acritarchs have been used as a biostratigraphical tool to correlate different regional sections of the Doushantuo Formation (e.g. Xiao 2004; C. Zhou *et al.* 2007; McFadden *et al.* 2009; C.-Y. Yin *et al.* 2009, 2011; Xiao *et al.* 2012, 2014a; Liu *et al.* 2014; Muscente *et al.* 2015). Since such fossils have yet to be revealed by our exploration of the Shuurgat Formation, we are unable to correlate Shuurgat strata with the Doushantuo sequence at the level of individual Doushantuo members.

The best-known fossils from the Doushantuo Formation are multicellular and mostly preserved in ore-grade phosphorites (Xiao *et al.* 1998, 2004, 2014a, b; Xiao & Knoll 2000; Xiao 2004). They include red algae (Xiao *et al.* 2004) and possible animal embryos (e.g. L. Chen *et al.* 2014). *Thallophycoides*, a multicellular form from the Doushantuo phosphorites interpreted as a stem group florideophyte (Xiao *et al.* 2004), has been reported from the basal Zuun-Arts phosphorites in Mongolia (Ragozina *et al.* 2007, 2016). The Shuurgat chert nodules, in contrast, have yielded no multicellular forms to date, with the possible exception of a single degraded specimen of a large spheroidal body containing loosely packed spheroids (Fig. 9H, I) which bears a resemblance to *Megasphaera* from Doushantuo. However, this poorly preserved single specimen is not sufficient evidence to show that the Shuurgat cherts preserve multicellular forms. Multicellular fossils are rare in the Doushantuo Formation (Y. Zhang *et al.* 1998; Xiao & Knoll 2000; Xiao 2004; Liu *et al.* 2014; Xiao *et al.* 2014a, b). Their absence in the Shuurgat cherts may therefore be a reflection of a different depositional environment and/or small sample size.

The Shuurgat sequence is variably phosphatized and often contains small phosphatic clasts that preserve

fossiliferous material, another parallel with Doushantuo. The small phosphatized areas in Shuurgat rocks may represent clasts of microbial mat. The preservation is poor and the organic material is often redistributed, distorting the morphology of the fossils. Furthermore, only unnamed simple filaments and spheroids are preserved. This contrasts with the spectacular preservation in the phosphorites of the Doushantuo Formation (e.g. Xiao *et al.* 1998, 2014a, b; Y. Zhang *et al.* 1998; Xiao & Knoll 2000; L. Chen *et al.* 2014; Muscente *et al.* 2015). While the Shuurgat sequence may not be an obvious target for phosphatized microfossils, exceptional fossils have been reported from the phosphorites of the basal Zuun-Arts Formation higher in the Mongolian sequence (Ragozina *et al.* 2007, 2010, 2016) which are more extensive stratigraphically and likely have a higher phosphate content. Fossils have also been reported from the late Ediacaran ore-grade phosphorites of the Khuvsgul Terrane of northern Mongolia (Zhegallo *et al.* 2000; Macdonald & Jones 2011), although their diversity has yet to be fully explored (Dorjnamjaa & Altanshagai 2015).

The similarity of the biota preserved in Shuurgat cherts to those of Doushantuo and Krol A cherts, in particular the presence of *Salome hubeiensis*, suggests regional biostratigraphical equivalence. The Shuurgat Formation thus provides a new window onto the early Ediacaran biological world and hints at the ecological complexity of Ediacaran communities, with the possible appearance of multicellular forms (?*Megasphaera*, Fig. 9H, I).

Conclusions

In addition to the discoveries described here, the Zavkhan Terrane has already yielded micro- and macrofossils of Cryogenian age (Bosak *et al.* 2011a, b; Serezhnikova *et al.* 2014; Cohen *et al.* 2015), and possible acanthomorphic/multicellular microfossils and macroscopic carbonaceous algal compressions from later Ediacaran rocks (Ragozina *et al.* 2007, 2010, 2016; Dornbos *et al.* 2016), as well as a diverse trace, small shelly and reefal fauna which flourishes into Cambrian time (e.g. Smith *et al.* 2016). This rich palaeobiological record, viewed in the context of new palaeoenvironmental and geochronological data (Bold *et al.* 2016; Smith *et al.* 2016), highlights the global importance of Mongolian sequences to our understanding of the transition from a microbial world to one containing complex metazoans.

Acknowledgements

This research benefitted from discussions with A. Knoll, L. Tarhan and S. Xiao. Students and staff at the School of Geology and Mining of the Mongolian University of

Science and Technology, C. Dwyer, T. Killian, E. Smith and E. F. Smith provided field assistance. S. Darroch assisted with statistical analyses of size frequency distributions. A. Hood advised on cathodoluminescence microscopy and provided valuable discussion. S. Butts and J. Utrup facilitated access to the collections of the Yale Peabody Museum of Natural History Division of Invertebrate Paleontology. We thank two anonymous reviewers for their constructive comments. This work was supported by the American Philosophical Society/National Aeronautics and Space Administration (NASA) Astrobiology Institute Lewis and Clark Fund for Exploration and Field Research in Astrobiology, a Geological Society of America ExxonMobil Student Geoscience Grant, the NASA Astrobiology Institute [NNA13AA90A] *Foundations of Complex Life, Evolution, Preservation and Detection on Earth and Beyond*, the Yale Institute for Biospheric Studies Small Grants Program, and the Yale Peabody Museum of Natural History. RPA was supported by NASA Headquarters under the Earth and Space Science Fellowship Program [NNX14AP10H].

ORCID

Ross P. Anderson  <http://orcid.org/0000-0002-0558-7563>

References

- Anderson, R. P., Fairchild, I. J., Tosca, N. J. & Knoll, A. H. 2013. Microstructures in metasedimentary rocks from the Neoproterozoic Bonahaven Formation, Scotland: Microconcretions, impact spherules, or microfossils? *Precambrian Research*, **233**, 59–72.
- Astashkin, V. A., Pegel, T. V., Repina, L. N., Belyaeva, G. V., Esakova, N. V., Rozanov, A. Y., Zhuravlev, A., Yu. Osadchaya, D. V. & Pakhomov, N. N. 1995. The Cambrian system of the foldbelts of Russia and Mongolia. *International Union of Geological Sciences*, **32**, 1–132.
- Bailey, J. V., Joye, S. B., Kalanetra, K. M., Flood, B. E. & Corsetti, F. A. 2007. Evidence of giant sulphur bacteria in Neoproterozoic phosphorites. *Nature*, **445**, 198–201.
- Barghoorn, E. S. & Tyler, S. A. 1965. Microorganisms from Gunflint Chert – these structurally preserved Precambrian fossils from Ontario are the most ancient organisms known. *Science*, **147**, 563–575.
- Bengtson, S., Cunningham, J. A., Yin, C. & Donoghue, P. C. J. 2012. A merciful death for the ‘earliest bilaterian’, Vernanimalcula. *Evolution and Development*, **14**, 421–427.
- Bold, U., Smith, E. F., Rooney, A. D., Bowring, S. A., Buchwaldt, R., Dudás, F. Ö., Ramezani, J., Crowley, J. L., Schrag, D. P. & Macdonald, F. A. 2016. Neoproterozoic stratigraphy of the Zavkhan Terrane of Mongolia: The backbone for Cryogenian and early Ediacaran chemostratigraphic records. *American Journal of Science*, **316**, 1–63.
- Bosak, T., Macdonald, F. Lahr, D. & Matys, E. 2011a. Putative Cryogenian ciliates from Mongolia. *Geology*, **39**, 1123–1126.

- Bosak, T., Lahr, D. J. G., Pruss, S. B., Macdonald, F. A., Dalton, L. & Matys, E.** 2011b. Agglutinated tests in post-Sturtian cap carbonates of Namibia and Mongolia. *Earth and Planetary Science Letters*, **308**, 29–40.
- Brasier, M. D., Green, O. & Shields, G.** 1997. Ediacaran sponge spicule clusters from southwestern Mongolia and the origins of the Cambrian fauna. *Geology*, **25**, 303–306.
- Brasier, M. D., Shields, G., Kuleshov, V. N. & Zhegallo, E. A.** 1996. Integrated chemo- and biostratigraphic calibration of early animal evolution: Neoproterozoic–early Cambrian of southwest Mongolia. *Geological Magazine*, **133**, 445–485.
- Briggs, D. E. G.** 2003. The role of decay and mineralization in the preservation of soft-bodied fossils. *Annual Review of Earth and Planetary Sciences*, **31**, 275–301.
- Briggs, D. E. G. & Kear, A. J.** 1993. Fossilization of soft tissue in the laboratory. *Science*, **259**, 1439–1442.
- Butterfield, N. J.** 2011. Terminal developments in Ediacaran embryology. *Science*, **334**, 1655–1656.
- Butterfield, N. J., Knoll, A. H. & Swett, K.** 1994. Paleobiology of the Neoproterozoic Svanbergfjellet Formation, Spitsbergen. *Fossils and Strata*, **34**, 1–84.
- Chen, J.-Y., Bottjer, D. J., Li, G., Hadfield, M. G., Gao, F., Cameron, A. R., Zhang, C.-Y., Xian, D.-C., Tafforeau, P., Liao, X. & Yin, Z.-J.** 2009. Complex embryos displaying bilaterian characters from Precambrian Doushantuo phosphate deposits, Weng'an, Guizhou, China. *Proceedings of the National Academy of Sciences*, **106**, 19056–19060.
- Chen, L., Xiao, S., Pang, K., Zhou, C. & Yuan, X.** 2014. Cell differentiation and germ-soma separation in Ediacaran animal embryo-like fossils. *Nature*, **516**, 238–241.
- Cohen, P. A. & Macdonald, F. A.** 2015. The Proterozoic record of eukaryotes. *Paleobiology*, **41**, 610–632.
- Cohen, P. A., Knoll, A. H. & Kodner, R. B.** 2009. Large spinose microfossils in Ediacaran rocks as resting stages of early animals. *Proceedings of the National Academy of Sciences*, **106**, 6519–6524.
- Cohen, P. A., Macdonald, F. A., Pruss, S., Matys, E. & Bosak, T.** 2015. Fossils of putative marine algae from the Cryogenian glacial interlude of Mongolia. *Palaios*, **30**, 238–247.
- Condon, D., Zhu, M., Bowring, S., Wang, W., Yang, A. & Jin, Y.** 2005. U-Pb ages from the Neoproterozoic Doushantuo Formation, China. *Science*, **308**, 95–98.
- Darroch, S. A. F., Laflamme, M. & Clapham, M. E.** 2013. Population structure of the oldest known macroscopic communities from Mistaken Point, Newfoundland. *Paleobiology*, **39**, 591–608.
- Dorjnamjaa, D. & Altanshagai, G.** 2015. Concerning the original viewpoint of biogeologic accumulation of the old bedded phosphorites in the Khubsugul and Zavkhan basins of Mongolia. *Open Journal of Geology*, **5**, 666–675.
- Dorjnamjaa, D. & Bat-Ireedui, Y.** 1991. Dokembriy Mongoliii. *Akademiya Nauk MPR, Geological Institute, Ulan Batar*, 182 pp.
- Dorjnamjaa, D., Bat-Ireedui, Y. A., Dashdavaa, Z. & Soelmaa, D.** 1993. Precambrian–Cambrian geology of the Zavkhan Zone. *Earth Sciences Department, University of Oxford*, Oxford, 36 pp.
- Dornbos, S. Q., Oji, T., Kanayama, A. & Gonchigdorj, S.** 2016. A new Burgess Shale-type deposit from the Ediacaran of western Mongolia. *Scientific Reports*, **6**, 23438.
- dos Reis, M., Thawornwattana, Y., Angelis, K., Telford, M. J., Donoghue, P. C. J. & Yang, Z.** 2015. Uncertainty in the timing of origin of animals and the limits of precision in molecular timescales. *Current Biology*, **25**, 2939–2950.
- Eisenack, A.** 1958. *Tasmanites* Newton 1875 und *Leiosphaeridia* n.g. als Gattungen de Hystrichosphaeridea. *Palaeontographica, Abteilung A*, **110**, 1–19.
- Endonzhams, Z. & Lkhasuren, B.** 1988. Stratigrafi ya pogrannichnykh tolsch dokembriya i kembriya Dzabkhanskoj zony. Pp. 150–162 in V. V. Khomentovsky & V. Y. Shenfil' (eds) *Pozdny dokembriy i ranniy paleozoy Sibiri, Rifey i vend. Institut Geologii i Geofiziki, Sibirskoe Otdelenie. Akademiya Nauk, SSSR, Novosibirsk*.
- Erwin, D. H., Laflamme, M., Tweedt, S. M., Sperling, E. A., Pisani, D. & Peterson, K. J.** 2011. The Cambrian conundrum: Early divergence and later ecological success in the early history of animals. *Science*, **334**, 1091–1097.
- Esakova, N. V. & Zhegallo, E. A.** 1996. Stratigrafaya i fauna nizhnego Kembriya Mongolii [Lower Cambrian stratigraphy and fauna of Mongolia]. *Sovmestnaya Sovetsko-Mongol'skaya Paleontologicheskaya Ekspeditsiya*, **46**, 208 pp.
- Fraley, C. & Raftery, A. E.** 2007. Bayesian regularization for normal mixture estimation and model-based clustering. *Journal of Classification*, **24**, 155–188.
- Gibsher, A. S. & Khomentovsky, V. V.** 1990. The sections of the Tsagan Oloom and Bayan Gol formations of the Vendian–Lower Cambrian in the Dzackhan zone of Mongolia. Pp. 79–91 in *Pozdny Dokembriy i Ranniy Paleozoy Sibiri Voprosy Regional'noy Stratigraphii*. Izdatelstvo Instituta Geologii i Geofiziki, Novosibirsk.
- Gibsher, A. S., Bat-Ireedui, Y. A., Balakhonov, I. G. & Efremenko, D. E.** 1991. The Bayan Gol reference section of the Vendian–Lower Cambrian in central Mongolia (subdivision and correlation). Pp. 107–120 in V. V. Khomentovsky (ed.) *Late Precambrian and Early Palaeozoic of Siberia. Siberian platform and its framework*. Ob'edinennyy Institut Geologii, Geofiziki i Mineralogii, Sibirskoe Otdelenie, Akademiya Nauk SSSR, Novosibirsk.
- Gold, D. A., Grabenstatter, J., de Mendoza, A., Riesgo, A., Ruiz-Trillo, I. & Summons, R. E.** 2016. Sterol and genomic analyses validate the sponge biomarker hypothesis. *Proceedings of the National Academy of Sciences*, **113**, 2684–2689.
- Goldring, R. & Jensen, S.** 1996. Trace fossils and biofabrics at the Precambrian–Cambrian boundary interval in western Mongolia. *Geological Magazine*, **133**, 403–415.
- Golub, I. N.** 1979. Novaya gruppa problematichnykh mikroobrazovanij v vendskikh otlozheniyakh Orshanskoj vpadiny (Russkaya platforma). [A new group of problematic microstructures in Vendian deposits of the Orshanka Basin (Russian Platform)]. Pp. 147–155 in B. S. Sokolov (ed.) *Paleontologiya Dokembriya i Rannego Kembriya*. Nauka, Leningrad.
- Golubkova, E. Y., Raevskaya, E. G. & Kuznetsov, A. B.** 2010. Lower Vendian microfossil assemblages of east Siberia: Significance for solving regional stratigraphic problems. *Stratigraphy and Geological Correlation*, **18**, 353–375.
- Grey, K.** 2005. Ediacaran palynology of Australia. *Memoirs of the Australasian Association of Palaeontologists*, **31**, 1–439.
- Hagadorn, J. W., Xiao, S., Donoghue, P. C. J., Bengtson, S., Gostling, N. J., Pawlowska, M., Raff, E. C., Raff, R. A., Turner, F. R., Chongyu, Y., Zhou, C., Yuan, X., McFeely, M. B., Stampanoni, M. & Neilson, K. H.** 2006. Cellular and subcellular structure of Neoproterozoic embryos. *Science*, **314**, 291–294.
- Halverson, G. P., Wade, B. P., Hurtgen, M. T. & Barovich, K. M.** 2010. Neoproterozoic chemostratigraphy. *Precambrian Research*, **182**, 337–350.
- Hermann, T. N.** 1974. Nakhodki massovykh skoplenij trikhomov v rifee. [Finds of massive accumulations of trichomes

- in the Riphean.]. Pp. 6–10 in B. V. Timofeev (ed.) *Mikrofito-fossilii Proterozoa i Rannego Paleozoa SSSR*. Nauka, Leningrad.
- Hoffman, P. F. & Schrag, D. P.** 2002. The Snowball Earth hypothesis: Testing the limits of global change. *Terra Nova*, **14**, 129–155.
- Hofmann, H. J.** 1976. Precambrian microflora, Belcher Islands, Canada: Significance and systematics. *Journal of Paleontology*, **50**, 1040–1073.
- Horodyski, R. J. & Donaldson, J. A.** 1980. Microfossils from the Middle Proterozoic Dismal Lakes Group, Arctic Canada. *Precambrian Research*, **11**, 125–159.
- Huldgren, T., Cunningham, J. A., Yin, C., Stampanoni, M., Marone, F., Donoghue, P. C. J. & Bengtson, S.** 2011. Fossilized nuclei and germination structures identify Ediacaran “animal embryos” as encysting protists. *Science*, **334**, 1696–1699.
- Jiang, G., Christie-Blick, N., Kaufman, A. J., Banerjee, D. M. & Rai, V.** 2002. Sequence stratigraphy of the Neoproterozoic Infra Krol Formation and Krol Group, Lesser Himalaya, India. *Journal of Sedimentary Research*, **72**, 524–542.
- Jiang, G., Christie-Blick, N., Kaufman, A. J., Banerjee, D. M. & Rai, V.** 2003. Carbonate platform growth and cyclicity at a terminal Proterozoic passive margin, Infra Krol Formation and Krol Group, Lesser Himalaya, India. *Sedimentology*, **50**, 921–952.
- Khomentovskiy, V. V. & Gibsher, A. S.** 1996. The Neoproterozoic–Lower Cambrian in northern Gobi-Altay, western Mongolia: Regional setting, lithostratigraphy and biostratigraphy. *Geological Magazine*, **133**, 371–390.
- Knoll, A. H.** 1981. Paleocology of late Precambrian microbial assemblages. Pp. 17–54 in K. Niklas (ed.) *Paleobotany, Paleocology, and Evolution*. Praeger, New York.
- Knoll, A. H.** 1982. Microfossils from the late Precambrian Draken conglomerate, NY Friesland, Svalbard. *Journal of Paleontology*, **56**, 755–790.
- Knoll, A. H.** 1985. Exceptional preservation of photosynthetic organisms in silicified carbonates and silicified peats. *Philosophical Transactions of the Royal Society of London, Series B*, **311**, 111–122.
- Knoll, A. H.** 1992. Vendian microfossils in metasedimentary cherts of the Scotia Group, Prins Karls Forland, Svalbard. *Palaeontology*, **35**, 751–774.
- Knoll, A. H.** 2003a. Biomineralization and evolutionary history. *Reviews in Mineralogy and Geochemistry*, **54**, 329–356.
- Knoll, A. H.** 2003b. *Life on a young planet: The first 3 billion years of evolution on Earth*. Princeton University Press, Princeton, 276 pp.
- Knoll, A. H.** 2012. The fossil record of microbial life. Pp. 297–314 in A. H. Knoll, D. E. Canfield & K. O. Konhauser (eds) *Fundamentals of geobiology*. Wiley Blackwell, Hoboken.
- Knoll, A. H.** 2014. Paleobiological perspectives on early eukaryotic evolution. *Cold Spring Harbor Perspectives in Biology*, **6**, 14 pp.
- Knoll, A. H.** 2015. Paleobiological perspectives on early microbial evolution. *Cold Spring Harbor Perspectives in Biology*, **7**, 17 pp.
- Knoll, A. H., Strother, P. K. & Rossi, S.** 1988. Distribution and diagenesis of microfossils from the Lower Proterozoic Duck Creek Dolomite, Western Australia. *Precambrian Research*, **38**, 257–279.
- Knoll, A. H., Swett, K. & Mark, J.** 1991. Paleobiology of a Neoproterozoic tidal flat/lagoonal complex: The Draken Conglomerate Formation, Spitsbergen. *Journal of Paleontology*, **65**, 531–570.
- Knoll, A. H., Javaux, E. J., Hewitt, D. & Cohen, P.** 2006. Eukaryotic organisms in Proterozoic oceans. *Philosophical Transactions of the Royal Society, Series B*, **361**, 1023–1038.
- Korobov, M. N.** 1980. Lower Cambrian biostratigraphy and miomeroid trilobites of the Lower Cambrian of Mongolia. Pp. 5–108 in V. V. Menner & S. V. Meyen (eds) *Lower Cambrian and Carboniferous biostratigraphy of Mongolia*. Trudy Sovmestnoy Sovetskogo-Mongol'skoy Paleontologicheskoy Ekspeditsii, Moscow.
- Korobov, M. N. & Missarzhevsky, V. V.** 1977. On the Cambrian and Precambrian boundary layers of western Mongolia. Pp. 7–9 in L. P. Tartarinov (ed.) *Palaeozoic Invertebrata of Mongolia*. Trudy Sovmestnaya Sovetsko-Mongol'skaya Paleontologicheskaya Ekspeditsiya, Moscow.
- Kruse, P. D., Gandin, A., Debrenne, F. & Wood, R.** 1996. Early Cambrian bioconstructions in the Zavkhan Basin of western Mongolia. *Geological Magazine*, **133**, 429–444.
- Li, Z.-X., Evans, D. A. D. & Halverson, G. P.** 2013. Neoproterozoic glaciations in a revised global palaeogeography from the breakup of Rodinia to the assembly of Gondwanaland. *Sedimentary Geology*, **294**, 219–232.
- Lindsay, J. F., Brasier, M. D., Dorjnamjaa, D., Goldring, R., Kruse, P. D. & Wood, R. A.** 1996. Facies and sequence controls on the appearance of the Cambrian biota in southwestern Mongolia: Implications for Precambrian–Cambrian boundary. *Geological Magazine*, **133**, 417–428.
- Liu, P., Xiao, S., Yin, C., Chen, S., Zhou, C. & Li, M.** 2014. Ediacaran acanthomorphic acritarchs and other microfossils from chert nodules of the Upper Doushantuo Formation in the Yangtze Gorges Area, South China. *Journal of Paleontology*, **88**, 1–139.
- Macdonald, F. A.** 2011. The Tsagaan Oloom Formation, southwestern Mongolia. Pp. 331–337 in E. Arnaud, G. P. Halverson & G. Shields-Zhou (eds) *The geological record of Neoproterozoic glaciations*. Geological Society of London, London.
- Macdonald, F. A. & Jones, D. S.** 2011. The Khubsugul Group, northern Mongolia. Pp. 339–345 in E. Arnaud, G. P. Halverson & G. Shields-Zhou (eds) *The geological record of Neoproterozoic glaciations*. Geological Society of London, London.
- Macdonald, F. A., Jones, D. S. & Schrag, D. P.** 2009. Stratigraphic and tectonic implications of a newly discovered glacial diamictite-cap carbonate couplet in southwestern Mongolia. *Geology*, **37**, 123–126.
- Maliva, R. G., Knoll, A. H. & Siever, R.** 1989. Secular change in chert distribution: A reflection of evolving biological participation in the silica cycle. *Palaios*, **4**, 519–532.
- Maloof, A. C., Porter, S. M., Moore, J. L., Dudás, F. Ö., Bowring, S. A., Higgins, J. A., Fike, D. A. & Eddy, M. P.** 2010. The earliest Cambrian record of animals and ocean geochemical change. *Geological Society of America Bulletin*, **122**, 1731–1774.
- McFadden, K. A., Xiao, S., Zhou, C. & Kowalewski, M.** 2009. Quantitative evaluation of the biostratigraphic distribution of acanthomorphic acritarchs in the Ediacaran Doushantuo Formation in the Yangtze Gorges area, South China. *Precambrian Research*, **173**, 170–190.
- Mendelson, C. V. & Schopf, J. W.** 1982. Proterozoic microfossils from the Sukhaya Tunguska, Shorikha, and Yudoma formations of the Siberian platform, USSR. *Journal of Paleontology*, **56**, 42–83.
- Muscente, A. D., Hawkins, A. D. & Xiao, S.** 2015. Fossil preservation through phosphatization and silicification in the

- Ediacaran Doushantuo Formation (South China): a comparative synthesis. *Palaeogeography, Palaeoclimatology, Palaeoecology*, **434**, 46–62.
- R Development Core Team** 2010. *R: a language and environment for statistical computing*. R Foundation for Statistical Computing, Vienna.
- Ragozina, A. L., Dorjnamjaa, D., Krayushkin, A. V. & Serezhnikova, E. A.** 2007. Body fossils and trace fossils from the Vendian–Cambrian section of Dzabkhan Zone Western Mongolia. Pp. 57–64 in M. A. Semikhatov (ed.) *The rise and fall of the Vendian (Ediacaran) Biota origin of a modern biosphere: proceedings of the international symposium (IGCP Project 493)*. GEOS, Moscow.
- Ragozina, A. L., Dorjnamjaa, D., Krayushkin, A. V., Serezhnikova, E. A. & Enkhbaator, B.** 2010. Vendian–Cambrian biota of the Western Mongolia. Pp. 187–190 in V. M. Podobina (ed.) *Evolution of life on the Earth: proceedings of the IV international symposium*. TML-Press, Tomsk.
- Ragozina, A. L., Dorjnamjaa, D., Serezhnikova, E. A., Zaitseva, L. V. & Enkhbaatar, B.** 2016. Association of macro- and microfossils in the Vendian (Ediacaran) postglacial successions in Western Mongolia. *Stratigraphy and Geological Correlation*, **24**, 242–251.
- Riedman, L. A., Porter, S. M., Halverson, G. P., Hurtgen, M. T. & Junium, C. K.** 2014. Organic-walled microfossil assemblages from glacial and interglacial Neoproterozoic units of Australia and Svalbard. *Geology*, **42**, 1011–1014.
- Rooney, A. D., Strauss, J. V., Brandon, A. D. & Macdonald, F. A.** 2015. A Cryogenian chronology: Two long-lasting synchronous Neoproterozoic glaciations. *Geology*, **43**, 459–462.
- Schiffbauer, J. D., Wallace, A. F., Broce, J. & Xiao, S.** 2014. Exceptional fossil preservation through phosphatization. *Paleontological Society Papers*, **20**, 59–82.
- Schopf, J. W.** 1968. Microflora of the Bitter Springs Formation, Late Precambrian, central Australia. *Journal of Paleontology*, **42**, 651–688.
- Schopf, J. W.** 2006. Fossil evidence of Archaean life. *Philosophical Transactions of the Royal Society, Series B*, **361**, 869–885.
- Schopf, J. W. & Klein, C.** 1992. *The Proterozoic biosphere: a multidisciplinary study*. Cambridge University Press, Cambridge, 1348 pp.
- Schopf, J. W., Sergeev, V. N. & Kudryavtsev, A. B.** 2015. A new approach to ancient microorganisms: Taxonomy, paleoecology, and biostratigraphy of the Lower Cambrian Berkuta and Chulaktau microbiotas of South Kazakhstan. *Journal of Paleontology*, **89**, 695–729.
- Serezhnikova, E. A., Ragozina, A. L., Dorjnamjaa, D. & Zaitseva, L. V.** 2014. Fossil microbial communities in Neoproterozoic interglacial rocks, Maikhanul Formation, Zavkhan basin, Western Mongolia. *Precambrian Research*, **245**, 66–79.
- Sergeev, V. N., Knoll, A. H. & Vorob'eva, N. G.** 2011. Ediacaran microfossils from the Ura Formation, Baikal–Patom uplift, Siberia: Taxonomy and biostratigraphic significance. *Journal of Paleontology*, **85**, 987–1011.
- Sergeev, V. N., Sharma, M. & Shukla, Y.** 2012. Proterozoic fossil cyanobacteria. *The Palaeobotanist*, **61**, 189–358.
- Smith, E. F., Macdonald, F. A., Petach, T. A., Bold, U. & Schrag, D. P.** 2016. Integrated stratigraphic, geochemical, and paleontological late Ediacaran to early Cambrian records from southwestern Mongolia. *Geological Society of America Bulletin*, **128**, 442–468.
- Tiwari, M. & Knoll, A. H.** 1994. Large acanthomorphic acritarchs from the Infrakrol Formation of the Lesser Himalaya and their stratigraphic significance. *Journal of Himalayan Geology*, **5**, 193–201.
- Ushatinskaya, G. T.** 1993. New genus of paterinid (brachiopod) from the Lower Cambrian of western Mongolia. *Paleontological Zhurnal*, **1**, 115–118.
- Valdiya, K. S.** 2016. Later Proterozoic and Early Cambrian in the Himalaya. Pp. 335–371 in K. S. Valdiya (ed.) *The making of India*. Springer International Publishing, Switzerland.
- Vorob'eva, N. G., Sergeev, V. N. & Knoll, A. H.** 2009. Neoproterozoic microfossils from the margin of the east European platform and the search for a biostratigraphic model of lower Ediacaran rocks. *Precambrian Research*, **173**, 163–169.
- Voronin, Y. L., Voronova, L. G., Grigor'eva, N. V., Drozdova, N. A., Zhegallo, E. A., Zhuravlev, A. Y., Ragozina, A. L., Rozanov, A. Y., Sayutina, T. A., Syosev, V. A. & Fonin, V. D.** 1982. The Precambrian/Cambrian boundary in the geosynclinal areas (the reference section of Salaany-Gol, MPR). *Trudy Sovmestnaya Sovetskogo-Mongol'skaya Paleontologicheskaya Ekspeditsiya, Akademia Nauk SSSR*, Moscow, 180 pp.
- Wood, R., Zhuravlev, A. Y. & Anaaz, C. T.** 1993. The ecology of Lower Cambrian buildups from Zuune Arts, Mongolia: Implications for early metazoan reef evolution. *Sedimentology*, **40**, 829–858.
- Xiao, S.** 2004. New multicellular algal fossils and acritarchs in Doushantuo chert nodules (Neoproterozoic; Yangtze Gorges, South China). *Journal of Paleontology*, **78**, 393–401.
- Xiao, S. & Knoll, A. H.** 2000. Phosphatized animal embryos from the Neoproterozoic Doushantuo Formation at Weng'an, Guizhou, South China. *Journal of Paleontology*, **74**, 767–788.
- Xiao, S. & Laflamme, M.** 2009. On the eve of animal radiation: phylogeny, ecology, and evolution of the Ediacara biota. *Trends in Ecology and Evolution*, **24**, 31–40.
- Xiao, S., Zhang, Y. & Knoll, A. H.** 1998. Three-dimensional preservation of algae and animal embryos in a Neoproterozoic phosphorite. *Nature*, **391**, 553–558.
- Xiao, S., Knoll, A. H., Yuan, X. & Pueschel, C. M.** 2004. Phosphatized multicellular algae in the Neoproterozoic Doushantuo formation, China, and the early evolution of florideophyte red algae. *American Journal of Botany*, **91**, 214–227.
- Xiao, S., Schiffbauer, J. D., McFadden, K. A. & Hunter, J.** 2010. Petrographic and SIMS pyrite sulfur isotope analyses of Ediacaran chert nodules: Implications for microbial processes in pyrite rim formation, silicification, and exceptional fossil preservation. *Earth and Planetary Science Letters*, **297**, 481–495.
- Xiao, S., Zhou, C., Liu, P., Wang, D. & Yuan, X.** 2014a. Phosphatized acanthomorphic acritarchs and related microfossils from the Ediacaran Doushantuo Formation at Weng'an (south China) and their implications for biostratigraphic correlation. *Journal of Paleontology*, **88**, 1–67.
- Xiao, S., McFadden, K. A., Peek, S., Kaufman, A. J., Zhou, C., Jiang, G. & Hu, J.** 2012. Integrated chemostratigraphy of the Doushantuo Formation at the northern Xiaofenghe section (Yangtze Gorges, South China) and its implication for Ediacaran stratigraphic correlation and ocean redox models. *Precambrian Research*, **192–195**, 125–141.
- Xiao, S., Muscente, A. D., Chen, L., Zhou, C., Schiffbauer, J. D., Wood, A. D., Polys, N. F. & Yuan, X.** 2014b. The Weng'an biota and the Ediacaran

- radiation of multicellular eukaryotes. *National Science Review*, **1**, 498–520.
- Xue, Y., Tang, T., Yu, C. & Zhou, C.** 1995. Large spheroidal chlorophyta fossils from the Doushantuo Formation phosphoritic sequence (late Sinian), central Guizhou, South China. *Acta Palaeontologica Sinica*, **34**, 688–706.
- Yao, W.-H., Li, Z.-X., Li, W.-X., Li, X.-H. & Yang, J.-H.** 2014. From Rodinia to Gondwanaland: A tale of detrital zircon provenance analyses from the southern Nanhua basin, South China. *American Journal of Science*, **314**, 278–313.
- Yin, C. & Liu, G.** 1988. Micropaleofloras of the Sinian system of Hubei. Pp. 91–100, 170–180 in Z. Zhao, Y. Xing, G. Ding & Y. Liu (eds) *The Sinian System of Hubei*. China University of Geosciences Press, Wuhan.
- Yin, C.-Y., Liu, P. J., Chen, S. M., Tang, F., Gao, L.-Z. & Wang, Z.-Q.** 2009. Acritarch biostratigraphic succession of the Ediacaran Doushantuo Formation in the Yangtze Gorges. *Acta Palaeontologica Sinica*, **48**, 146–154.
- Yin, C., Liu, P., Awramik, S. M., Chen, S., Tang, F., Gao, L., Wang, Z. & Riedman, L. A.** 2011. Acanthomorph biostratigraphic succession of the Ediacaran Doushantuo Formation in the East Yangtze Gorges, South China. *Acta Geologica Sinica*, **85**, 283–295.
- Yin, L., Zhu, M., Knoll, A. H., Yuan, X., Zhang, J. & Hu, J.** 2007. Doushantuo embryos preserved inside diapause egg cysts. *Nature*, **446**, 661–663.
- Yin, Z., Zhu, M., Tafforeau, P., Chen, J., Liu, P. & Li, G.** 2013. Early embryogenesis of potential bilaterian animals with polar lobe formation from the Ediacaran Weng'an Biot, South China. *Precambrian Research*, **225**, 44–57.
- Yuan, X., Chen, Z., Xiao, S., Zhou, C. & Hua, H.** 2011. An early Ediacaran assemblage of macroscopic and morphologically differentiated eukaryotes. *Nature*, **470**, 390–393.
- Zang, W. & Walter, M. R.** 1992. Late Proterozoic and Cambrian microfossils and biostratigraphy, Amadeus Basin, central Australia. *Association of Australian Palaeontologists, Memoir*, **12**, 1–132.
- Zhang, Y., Yin, L., Xiao, S. & Knoll, A. H.** 1998. Permineralized fossils from the terminal Proterozoic Doushantuo Formation, South China. *Paleontological Society Memoir*, **50**, 1–52.
- Zhang, Z.** 1984. A new microphytoplankton species from the Sinian of western Hubei province. *Acta Botanica Sinica*, **26**, 94–98.
- Zhang, Z.** 1986. New material of filamentous fossil cyanophytes from the Doushantuo Formation (Late Sinian) in the eastern Yangtze Gorges. *Scientia Geologica Sinica*, **1**, 30–37.
- Zhegallo, E. A., Rozanov, A. Y., Ushatinskaya, G. T., Hoover, R. B., Gerasimenko, L. M. & Ragozina, A. L.** 2000. *Atlas of microorganisms from ancient phosphorites of Khubsugul (Mongolia)*. Paleontological Institute of Russian Academy of Sciences & NASA-Marshall Space Flight Center, Huntsville, 167 pp.
- Zhou, C., Xie, G., McFadden, K., Xiao, S. & Yuan, X.** 2007. The diversification and extinction of Doushantuo-Pertataka acritarchs in South China: Causes and biostratigraphic significance. *Geological Journal*, **42**, 229–262.
- Zhou, C.-M., Yuan, X.-L. & Xue, Y.-S.** 1998. Sponge spicule-like pseudofossils from the Neoproterozoic Toudoushan formation in Weng'an, Guizhou, China. *Acta Micropalaeontologica Sinica*, **15**, 380–384.